World Journal of Stem Cells

Submit a Manuscript: https://www.f6publishing.com

World J Stem Cells 2021 January 26; 13(1): 91-114

DOI: 10.4252/wjsc.v13.i1.91

ISSN 1948-0210 (online)

ORIGINAL ARTICLE

Basic Study

Vascularization and osteogenesis in ectopically implanted bone tissue-engineered constructs with endothelial and osteogenic differentiated adipose-derived stem cells

Jelena G Najdanović, Vladimir J Cvetković, Sanja T Stojanović, Marija Đ Vukelić-Nikolić, Jelena M Živković, Stevo J Najman

ORCID number: Jelena G Najdanović 0000-0003-4178-3913; Vladimir J Cvetković 0000-0002-7462-310X; Sanja T Stojanović 0000-0002-6560-6762; Marija Đ Vukelić-Nikolić 0000-0002-2405-5140; Jelena M Živković 0000-0002-4010-5742; Stevo J Najman 0000-0002-2411-9802.

Author contributions: Najman SJ conceptualized the original idea and designed and coordinated the research study; Najdanović JG and Cvetković VJ performed the research and acquired the data; Najdanović JG, Cvetković VJ, Stojanović ST and Najman SJ analyzed and interpreted the data; Stojanović ST and Vukelić-Nikolić MD contributed new analytic tools; Najdanović JG and Cvetković VJ drafted and wrote the manuscript; Najdanović JG, Cvetković VJ, Stojanović ST, Vukelić-Nikolić MD, Živković JM and Najman SJ made critical revisions to the manuscript; All authors have read and approved the final manuscript.

Supported by Ministry of Education, Science and Technological Development of the Republic of Serbia, No. III 41017.

Institutional review board

Jelena G Najdanović, Sanja T Stojanović, Stevo J Najman, Department of Biology and Human Genetics; Department for Cell and Tissue Engineering, Faculty of Medicine, University of Niš, Niš 18108, Serbia

Vladimir J Cvetković, Department of Biology and Ecology, Faculty of Sciences and Mathematics, University of Niš, Niš 18106, Serbia

Marija Đ Vukelić-Nikolić, Jelena M Živković, Department of Biology and Human Genetics; Scientific Research Center for Biomedicine; Faculty of Medicine, University of Niš, Niš 18108, Serbia

Corresponding author: Stevo J Najman, PhD, Full Professor, Department of Biology and Human Genetics; Department for Cell and Tissue Engineering, Faculty of Medicine, University of Niš, Blvd. Dr Zorana Djindjica 81, Niš 18108, Serbia. stevo.najman@medfak.ni.ac.rs

Abstract

BACKGROUND

A major problem in the healing of bone defects is insufficient or absent blood supply within the defect. To overcome this challenging problem, a plethora of approaches within bone tissue engineering have been developed recently. Bearing in mind that the interplay of various diffusible factors released by endothelial cells (ECs) and osteoblasts (OBs) have a pivotal role in bone growth and regeneration and that adjacent ECs and OBs also communicate directly through gap junctions, we set the focus on the simultaneous application of these cell types together with platelet-rich plasma (PRP) as a growth factor reservoir within ectopic bone tissue engineering constructs.

AIM

To vascularize and examine osteogenesis in bone tissue engineering constructs enriched with PRP and adipose-derived stem cells (ASCs) induced into ECs and OBs.

METHODS

ASCs isolated from adipose tissue, induced *in vitro* into ECs, OBs or just expanded were used for implant construction as followed: BPEO, endothelial and osteogenic

statement: This study was approved by Faculty of Medicine, University of Niš, Laboratory for Cell Culture of Institute for Biomedical Research, Head of the Laboratory for Cell Culture: Prof. Dr. Stevo Najman, approval No. 01/5150 (16.09.08).

Institutional animal care and use committee statement: All animal procedures in this experiment were performed in accordance with the Animal Welfare Act (Republic of Serbia), which is in compliance with European Union guidelines for experimental animals. The animal procedures were approved by the Institutional Ethics Committee of the Faculty of Medicine, University of Niš, Serbia, approval No. 01-2857-8.

Conflict-of-interest statement: The authors have no potential conflicts of interest to declare.

Data sharing statement: Technical appendix, statistical code, and dataset available from the corresponding author at the email address stevo.najman@medfak.ni.ac.rs.

ARRIVE guidelines statement: The authors have read the ARRIVE Guidelines, and the manuscript was prepared and revised according to the ARRIVE Guidelines.

Manuscript source: Invited manuscript

differentiated ASCs with PRP and bone mineral matrix; BPUI, uninduced ASCs with PRP and bone mineral matrix; BC (control), only bone mineral matrix. At 1, 2, 4 and 8 wk after subcutaneous implantation in mice, implants were extracted and endothelial-related and bone-related gene expression were analyzed, while histological analyses were performed after 2 and 8 wk.

RESULTS

The percentage of vascularization was significantly higher in BC compared to BPUI and BPEO constructs 2 and 8 wk after implantation. BC had the lowest endothelial-related gene expression, weaker osteocalcin immunoexpression and *Spp1* expression compared to BPUI and BPEO. Endothelial-related gene expression and osteocalcin immunoexpression were higher in BPUI compared to BC and BPEO. BPEO had a higher percentage of vascularization compared to BPUI and the highest CD31 immunoexpression among examined constructs. Except *Vwf*, endothelial-related gene expression in BPEO had a later onset and was upregulated and well-balanced during *in vivo* incubation that induced late onset of *Spp1* expression and pronounced osteocalcin immunoexpression at 2 and 8 wk. Tissue regression was noticed in BPEO constructs after 8 wk.

CONCLUSION

Ectopically implanted BPEO constructs had a favorable impact on vascularization and osteogenesis, but tissue regression imposed the need for discovering a more optimal EC/OB ratio prior to considerations for clinical applications.

Key Words: Adipose-derived stem cells; Endothelial-related genes; Bone-related genes; Ectopic osteogenesis; Vascularization; Platelet-rich plasma

Core Tip: For successful bone regeneration, osteogenesis and vasculogenesis should be supported by the appropriate combination of cells, growth factors and biomaterials (biological triad). Because the optimal triad composition is unknown, our aim was to combine endothelial and osteogenic differentiated adipose-derived stem cells in the same construct with platelet-rich plasma on bone mineral matrix as a carrier. This construct was examined in a mouse subcutaneous implantation model that enabled interplay between endothelial cells and osteoblasts in induction of ectopic osteogenesis. The results indicated the potential of this approach, but further preclinical evaluations in orthotopic model regarding optimization of ECs/OBs ratio are necessary.

Citation: Najdanović JG, Cvetković VJ, Stojanović ST, Vukelić-Nikolić MĐ, Živković JM, Najman SJ. Vascularization and osteogenesis in ectopically implanted bone tissue-engineered constructs with endothelial and osteogenic differentiated adipose-derived stem cells. *World J Stem Cells* 2021; 13(1): 91-114
URL: https://www.wjgnet.com/1948-0210/full/v13/i1/91.htm
DOI: https://dx.doi.org/10.4252/wjsc.v13.i1.91

INTRODUCTION

Bone tissue is composed of various types of bone specialized cells, blood vessels and mineralized collagen fibers that are organized in hierarchical order[1]. This tissue has excellent self-regeneration capacity and capability of generating a new blood vessel network[2]. Natural healing involves three consecutive steps: Inflammation; osteogenesis; and bone remodeling[3].

Congenital skeletal abnormalities, trauma, removal of cancer tissue or infections remarkably reduce bone regeneration capacity due to insufficient or absent blood vessels within the defect[4] that further causes a lack of oxygen and nutrition supply and metabolic waste removal[5]. As a consequence, cell viability around the bone defect is low, and cells die[6,7]. To overcome the challenging problem of poor vascularization within the bone defect, a plethora of approaches have been developed in the field of

Specialty type: Cell and tissue engineering

Country/Territory of origin: Serbia

Peer-review report's scientific quality classification

Grade A (Excellent): A
Grade B (Very good): 0
Grade C (Good): C
Grade D (Fair): 0
Grade E (Poor): 0

Received: July 12, 2020
Peer-review started: July 12, 2020
First decision: September 24, 2020
Revised: November 1, 2020
Accepted: November 17, 2020
Article in press: November 17, 2020
Published online: January 26, 2021

P-Reviewer: Dai J, Yong KW
S-Editor: Huang P
L-Editor: Filipodia
P-Editor: Li X

bone tissue engineering (BTE). Bearing in mind that the interplay of various diffusible factors released by endothelial cells (ECs) and osteoblasts (OBs) have a pivotal role in bone growth and regeneration[8] and that adjacent ECs and OBs also communicate directly by proteins at gap junctions[9], we set the focus on the simultaneous application of these two cells types within BTE constructs.

In order to obtain a sustainable source of ECs and OBs, adipose tissue is one of the options. Adipose tissue consists mainly of mature adipocytes (90%), but it also contains a stromal vascular fraction (SVF), which is attractive for the application in bone regenerative medicine and in BTE[10]. SVF is composed of a heterogeneous population of cells, including preadipocytes, EC progenitors, pericytes, fibroblasts, mast cells and macrophages, and about 2% is adipose-derived stem cells (ASCs)[10]. SVF can be applied directly[11-13], or ASCs can be induced *in vitro* towards various cell types, including ECs and OBs[11,14-17]. Absence of HLA-DR expression makes ASCs suitable for allogenic applications[18].

Two types of interactions are crucial for the development of BTE constructs. The first one is the interaction between ECs and OBs, and the second is the interaction of these types of cells with biomaterial[5]. Besides cells and biomaterials, a source of regulatory molecules that have an influence on both ECs and OBs is essential for BTE constructs. There are studies regarding the improvement of vascularization and osteogenesis in BTE constructs that include the simultaneous application of ECs and OBs. However, their outcome varies depending on the applied experimental model, experimental animals, biomaterial, EC/OB ratio and source of growth factors or conditions. When ASCs were differentiated *in vitro* into ECs and OBs and seeded onto polylactic acid gas-plasma-treated scaffolds, applied as monocultures or co-cultures in ratio 1:1 and implanted into critical-sized rat calvarial defect, vascularization was enhanced in the ECs monoculture group, and osteogenesis was enhanced in both monoculture groups. However, the coculture group did not enhance the vascularization and osteogenesis compared to the group containing undifferentiated ASCs[19]. Similarly, cocultivated ECs and OBs combined and applied with sterilized and decellularized banked rat calvaria allografts have not brought success[20]. However, it has been revealed that vascularization within critical-sized calvarial defects is more advanced when the allografts were seeded with EC monocultures compared to the allografts seeded with OB monocultures and allografts seeded with EC/OB cocultures[20].

Great success has been accomplished in another orthotopic model of critical-sized bone defects in rat femur where mesoporous bioactive glass scaffolds were pre-vascularized with ASCs induced into ECs and subsequently seeded with ASCs induced into OBs[21]. These constructs improved angiogenesis and induced a higher mineral deposition rate in comparison with mesoporous bioactive glass seeded with osteogenic differentiated ASCs and unseeded mesoporous bioactive glass scaffolds. When it comes to ectopic osteogenesis models, double cell sheets of endothelial and osteogenic differentiated ASCs combined with coral hydroxyapatite, where EC sheets were inside and OB sheets were outside coral hydroxyapatite, were shown to have more advanced vascularization and osteogenesis compared to other types of coral hydroxyapatite-double cell sheet constructs[22]. *In vitro* cocultivated endothelial and osteogenic differentiated ASCs seeded together with CD14+ osteoclast progenitors onto HA/bTCP scaffolds were implanted subcutaneously into nude mice dorsal pockets and have shown a favorable effect on vascularization and bone-like tissue formation 3 wk after implantation[23].

In the above-cited studies, there is no unique answer that can be given about the optimal composition of BTE constructs. It is unequivocally clear that the appropriate combination of biomaterial triad components (cells, growth factors and biomaterials) have to be found. To the best of our knowledge, there are no data regarding endothelial-related gene expression and the dynamic of this expression related to osteogenesis in ectopic BTE constructs containing both endothelial and osteogenic differentiated ASCs combined with platelet-rich plasma (PRP) and biomaterials carrier. Our aim was to examine the effects of simultaneously applied endothelial and osteogenic differentiated ASCs combined with PRP and delivered on the bone mineral matrix (BMM) on vascularization and osteogenesis in ectopically implanted BTE constructs. To examine the importance of *in vitro* endothelial and osteogenic induction, BTE constructs containing uninduced ASCs, PRP and BMM were also prepared. BMM-only constructs represented a basic group of constructs that served as a carrier control.

MATERIALS AND METHODS

Institutional animal care and use committee statement

All animal procedures in this experiment were performed in accordance with the Animal Welfare Act (Republic of Serbia), which is in compliance with European Union guidelines for experimental animals. The animal procedures were approved by the Institutional Ethics Committee of the Faculty of Medicine, University of Niš, Serbia, approval No. 01-2857-8.

Experimental animals

The animal protocol was designed to minimize pain or discomfort to the animals. Adult, syngeneic, healthy male BALB/c mice weighing 22-24 g and 8-weeks-old were used in this study. Mice were held in standard laboratory conditions at 25 °C and 12 h light/12 h dark regime with an *ad libitum* access to food and water.

BMM

Deproteinized sterilized bovine bone, Bio-Oss®(Geistlich-Pharma, Wolhusen, Switzerland), with granules 0.25-1 mm in size (size S) was used for the implant construction. Due to its biocompatibility, osteoconductivity, highly interconnected pores, high surface area[24] and high structural similarity to hydroxyapatite in bone[25], this biomaterial is suitable as a carrier for growth factors and cells. In the present study, Bio-Oss® was used as a carrier for cells and growth factors and therefore labeled as BMM carrier.

PRP

PRP used for the implant construction was prepared in a two-step method. First, blood taken from mice orbital sinus according to the previously described technique[26] was collected into tubes that contained anticoagulant 4% sodium citrate and centrifuged for 10 min at room temperature. In the first centrifugation step, the supernatant containing plasma with platelets was collected and centrifuged for another 10 min. After the second centrifugation step, the pellet with platelets was resuspended in a small volume of supernatant plasma to get 4-5 higher concentration of platelets in PRP than physiological[27]. The number of platelets established in Malassez chamber (Paul Marienfeld GmbH & Co. KG, Lauda-Königshofen, Germany) was $1.89 \times 10^6 \pm 0.5 \times 10^6$ platelets per microliter of PRP. The final concentration of applied PRP in the liquid component of the implants was 10% (v/v), which was reported as the optimal concentration for combining with mesenchymal stem cells (MSCs)[28,29]. One aliquot of PRP was stored in RNA stabilization solution RNAlater® (Ambion, Life Technologies, Paisley, United Kingdom) for RNA isolation step and further used as calibrator sample in quantitative real-time (qRT)-PCR analysis.

Isolation and cultivation of ASCs

ASCs were obtained from SVF of visceral epididymal adipose tissue of BALB/c mice, according to a previously established protocol[10,15,16,30,31]. Briefly, extracted, washed and macerated tissue was digested (45 min, at 37 °C) using collagenase type I (Sigma-Aldrich, Hamburg, Germany) dissolved at the concentration of 2000 IU per 1 mL in Dulbecco's Modified Eagles Minimal Essential Medium (DMEM, PAA Laboratories GmbH, Pasching, Austria). Digested tissue was passed through a 180 μm mesh and centrifuged (10 min, 1500 rpm, 4 °C) upon which the lipid "ring" from the top of the tube and the middle portion were removed. The remaining pellet containing ASCs was seeded among 25 cm^2 cell culture flasks (Greiner Bio-One, Frickenhausen, Germany) at a density of 1×10^6 in complete DMEM (cDMEM), which is DMEM supplemented with 10% fetal bovine serum (FBS, PAA Laboratories GmbH, Pasching, Austria), 2 mmol/L L-glutamine (PAA Laboratories GmbH, Pasching, Austria) and 1% antibiotic-antimycotic solution (PAA Laboratories GmbH) that contained 100 IU/mL penicillin, 100 μg/mL streptomycin and 125 ng/mL amphotericin B. Cells were monitored daily on inverted light microscope Axio Observer.Z1 (Carl Zeiss, Oberkochen, Germany) equipped with the camera AxioCam HR (Carl Zeiss).

The cells were cultivated in cDMEM in standard cell culture conditions at a temperature of 37 °C in humified atmosphere and in a presence of 5% CO_2. The medium was changed every 2-3 d to discard nonattached cells. Upon achieving 80% confluence, the cells were passaged using trypsin/EDTA solution (PAA Laboratories, GmbH). The cells were cultivated in cDMEM up to the third passage (P03) in order to purify the MSCs from the other cell types contained within the SVF. One day after the P03, RNA stabilization solution, RNAlater®, was added to one aliquot of cells. These

cells were labeled as P03-1d cells, stored at -80 °C until RNA isolation and used as calibrator samples in qRT-PCR analysis.

Endothelial and osteogenic differentiation of ASCs

At P03, the cells counted using Trypan blue dye-exclusion method were seeded into 24-well plates (Greiner Bio-One, Frickenhausen, Germany) at a density of 0.5×10^4 per well. Three types of cell culture were established: (1) Endothelial differentiated ASCs. Endothelial differentiation was induced by using complete endoprime medium that was prepared by mixing components of EndoPrime Kit (PAA Laboratories GmbH, Austria), 5% FBS and 1% antibiotic-antimycotic solution. Complete endoprime medium, 2 mL in each well, consisted of 500 mL Base Medium, 5 mL EndoPrime supplement, 1 mL vascular endothelial growth factor (VEGF), 1 mL epidermal growth factor, 25 mL FBS, 2 mmol/L L-glutamine, 100 IU/mL penicillin, 100 μg/mL streptomycin and 125 ng/mL amphotericin B; (2) Osteogenic differentiated ASCs. Osteogenic differentiation was induced by using osteogenic media. Osteogenic media, 2 mL in each well, was prepared by mixing 500 mL of cDMEM, 1×10^{-8} mol/L dexamethasone, 50 μg/mL ascorbic acid and 10 mmol/L β-glycerophosphate; and (3) Uninduced ASCs. These cells were cultivated in cDMEM, 2 mL in each well, until the 12th day after the third passage (labeled as P03-12d cells). For gene expression analysis, P03-12d cells were placed into RNAlater® and stored at -80 °C.

In our earlier studies, we established that relative expression levels of endothelial-related genes in endothelial differentiated ASCs was the highest at the 12th day of endothelial differentiation[16] and that relative expression levels of bone-related genes were the highest at the 15th day of osteogenic differentiation[15]. In the present study, the same expression pattern was observed in both types of induced ASCs (data not shown). Therefore, we have applied ASCs at the 12th day of endothelial differentiation and ASCs at the 15th day of osteogenic differentiation for the implant construction.

Preparation of implants and implantation procedure

All implants were composed from 20 μL of liquid component and 10 mg (approximately 0.02 cm^3) of BMM. Three types of implants were constructed: (1) BPEO, composed of 0.5×10^4 ECs (obtained after 12 d of *in vitro* endothelial differentiation of ASCs) in 9 μL of DMEM, 0.5×10^4 OBs (obtained after 15 d of *in vitro* osteogenic differentiation of ASCs) in 9 μL of DMEM, 2 μL of PRP (finally 10% v/v) as a liquid component and 10 mg of BMM; (2) BPUI, composed of 1×10^4 P03-12d cells in 18 μL of DMEM and 2 μL of PRP (finally 10% v/v) as a liquid component and 10 mg of BMM; and (3) BC (carrier-control group), composed of 20 μL of DMEM as a liquid component and 10 mg of BMM.

Before implantation, PRP used for the implant construction was activated with calcium chloride, mixed with cell suspensions and quickly loaded onto BMM granules. The cells were allowed to attach to the BMM surface for 10-15 min[32], which also allowed for fibrin fibers to form. Each single implant was shaped into a lump after clotting[25].

Seventy-two BALB/c mice were randomly divided into three groups (BPEO, BPUI and BC) that consisted of twenty-four animals each. Mice were anesthetized by peritoneal administration of ketamine hydrochloride according to the guidelines for mice anesthesia. Surgical fields were cleaned with povidone-iodine solution, and mice were shaved. Implants were placed ectopically into interscapular subcutaneous tissue with a large, sterile biopsy needle. After the implantation procedure, surgical fields were cleaned again with povidone-iodine solution.

Each animal carried four implants of the same type. At 1, 2, 4 and 8 wk (*in vivo* experimental periods) after implantation procedure, six animals were sacrificed per group per time point. Implants extracted after each *in vivo* experimental period were stored in RNAlater® at -80 °C until several endothelial-related and one bone-related gene expression analysis, while implants extracted after 2 and 8 wk of *in vivo* experimental period were also placed in 10% neutral buffered formalin (NBF) for subsequent histological analysis.

Gene expression analysis

Endothelial-related gene expression was examined in P03-12d cells. To assess whether simultaneously applied endothelial and osteogenic differentiated ASCs combined with PRP have an impact on vascularization and osteogenesis in ectopically implanted BTE construct, relative expression of four endothelial-related and one bone-related gene was examined.

Total RNA from cultivated cells and extracted implants was isolated using the

RNeasy Mini Kit® (Qiagen, Hilden, Germany) according to the manufacturer's instructions. For residual DNA on-column digestion, DNase I RNase-free set (Qiagen) was applied according to the manufacturer's instructions. Immediately after RNA isolation, the concentration of RNA in the samples was determined according to the manufacturer's instructions using Qubit® 2.0 fluorometer and Qubit® RNA assay kit (Invitrogen, Thermo Fisher Scientific, Waltham, MA, United States).

Isolated total RNA was reverse transcribed into single-stranded cDNA using High-capacity cDNA Reverse Transcription Kit (Applied Biosystems®, Thermo Fisher Scientific, Waltham, MA, United States) according to the manufacturer's protocol. Reactions were performed in three steps (10 min at 25 °C; 120 min at 37 °C, and 5 min at 85 °C), in a SureCycler 8800 (SureCycler8800; Agilent Technologies, Santa Clara, CA, United States).

The relative expression level of endothelial-related genes in P03-12d cells was determined regarding the expression levels of the same genes in the cell culture established 1 d after the third passage (labeled as: P03-1d cells, calibrator sample). The relative expression level of endothelial-related genes and one bone-related gene in the implants was determined regarding expression of the same genes in the P03-1d cells combined with PRP (calibrator sample).

Gene expression was quantified by qRT-PCR using Kapa Sybr® Fast Universal qPCR Master Mix (2 ×) kit (Kapa Biosystems, Wilmington, MA, United States) in accordance with the manufacturer's recommendation. Amplification was performed, monitored and analyzed by a RealTime thermal cycler and its software Stratagene MxPro-Mx3005P (Agilent Technologies, Santa Clara, CA, United States). Amplification reactions were performed for 40 cycles. The following thermal profile was set for each cycle: enzyme activation for 3 min at 95 °C; denaturation 3 s at 95 °C; annealing 20 s at 55 °C; and extension 1 s at 72 °C. Primer-dimer presence and specificity and quality of PCR products were performed after 40 cycles of the amplification reaction by melting curve analysis (ramp from 55 °C to 95 °C). Commercially available primers for mice (Quantitect primer assays; Qiagen) were used for target genes (Table 1). Relative gene expression in all samples, including calibrator samples, was normalized to the housekeeping gene, β-actin, which was used as an endogenous control.

Histology and histomorphometry

The implants extracted 2 and 8 wk after implantations that were placed in 10% neutral buffered formalin were decalcified in 10% EDTA solution (pH 7.4), dehydrated in ascending concentrations of ethanol and embedded in paraffin. Paraffin tissue blocks were sectioned (4 μm) on a microtome Leica RM2235 (Leica Microsystems, Solms, Germany). Obtained tissue sections were deparaffinized with xylene and stained with hematoxylin and eosin and Masson's trichrome stains. Stained sections were analyzed under light microscope LEICA DMR and imaged using a LEICA DC 300 camera.

Histomorphometric measurements were performed in the NIS-Elements software version 3.2 (Nikon, Tokyo, Japan) on hematoxylin and eosin stained tissue sections. The images were obtained on a microscope Leica DMLS equipped with the camera CMEX-10 Pro (Euromex Microscopen BV, Netherlands) at 100 × magnification. The total area of implants and the total area of blood vessels were measured using the "Annotations and Measurements" tool in the software. The percentage of vascularization (%) was calculated as follows: (total vessel area/total area of implants) × 100.

Immunohistochemistry

The implants extracted 2 and 8 wk after implantation that were placed in 10% neutral buffered formalin were decalcified in 10% EDTA solution (pH 7.4), dehydrated in ascending concentrations of ethanol, embedded in paraffin and sliced at 4 μm on a microtome Leica RM2235. Tissue sections were further deparaffinized. To unmask antigenic sites, antigen-retrieval process was performed using 10 mmol/L sodium citrate buffer (pH 6.0) in the microwave oven prewarmed at 96 °C. After that, tissue sections were left at room temperature for 30 min to cool off.

Rabbit specific HRP/DAB detection kit (ab64261, Abcam, Cambridge, United Kingdom) was used for visualization according to the manufacturer's instruction. This kit contains: 0.3% Hydrogen Peroxide Block, Protein Block, Biotinylated goat anti-rabbit IgG, Streptavidin Peroxidase, DAB substrate and DAB chromogen. First, Hydrogen Peroxide Block was applied (10 min, room temperature) to block endogenous peroxidase activity, and then the tissue sections were treated with Protein Block (5 min, room temperature) to abolish nonspecific binding of the primary antibodies. After this step, tissue sections were incubated with the following primary antibodies overnight at 4 °C: anti-VEGFR-2 (ab2349; Abcam, Cambridge, United

Table 1 List of the primers used for quantitative real-time PCR

Gene name (abbreviation)	QuantiTect primer assay
β-actin (*Actb*)	Mm_Actb_2_SG, QT01136772
von Willebrand factor (*Vwf*)	Mm_Vwf_1_SG, QT00116795
Early growth response 1 (*Egr1*)	Mm_Egr1_1_SG, QT00265846
Vascular endothelial growth factor receptor 1 (*Flt1*)	Mm_Flt1_1_SG, QT00096292
Vascular cell adhesion molecule 1 (*Vcam1*)	Mm_Vcam1_1_SG, QT00128793
Osteopontin (*Spp1*)	Mm_Spp1_1_SG, QT00157724

Kingdom) at a dilution of 1:200; anti-CD31 (PAA363Mu01; Cloud-Clone Corp., Houston, TX, United States) at a dilution of 1:1000; and anti-osteocalcin (ab9386; Abcam) at a dilution of 1:200. Negative controls were the sections prepared in the same way but primary antibodies were omitted.

Further, the sections were incubated with Biotinylated goat anti-rabbit IgG (10 min, room temperature), Streptavidin Peroxidase (10 min, room temperature) and DAB chromogen mixed with DAB substrate (10 min, room temperature). The sections were counterstained with Mayer's Hematoxylin (5 min, room temperature), rinsed in tap-water, dehydrated and mounted (VectaMount®; Vector Laboratories, Burlingame, CA). Stained sections were analyzed and imaged on a light microscope LEICA DMR equipped with LEICA DC 300 camera.

To quantify VEGFR-2, CD31 and osteocalcin immunoexpression, ImageJ free software version 1.53 (National Institute of Health, Bethesda, MD, United States) (Java 1.8.0_172) was used. Tissue sections were imaged on a light microscope LEICA DMR equipped with LEICA DC 300 camera, at 40 × objective magnification. The immunohistochemistry (IHC) optical density (OD) score was applied to validate the intensity of VEGFR-2, CD31 and osteocalcin immunoexpression in the infiltrated tissue according to a previously established protocol[33] by using the open source plugin IHC profiler in the ImageJ software. Because OD is relative to the concentration of the applied stain (Lambert–Beer law)[34] the amount of detected stain determines the OD at a wavelength specific for the stain. We applied hematoxylin and DAB for IHC staining, and the IHC profiler developed by Varghese *et al*[35] was suitable for our IHC sections.

The IHC profiler automatically counts the semiquantitative OD score that corresponds to the intensity of each pixel ranked from negative to highly positive[36]. Semiquantitative data were converted into a quantitative result by using the following formula adapted from Seyed Jafari *et al*[33]: IHC OD score = percentage contribution of high positive × 4 + percentage contribution of positive × 3 + percentage contribution of low positive × 2 + percentage contribution of negative × 1.

Under 40 × objective magnification, five regions of interest (per group/per antibody/per experimental period) were selected randomly in IHC-stained sections to count the average IHC OD score. IHC OD in the sections was analyzed only in the infiltrated tissue with granules excluded.

Statistical analysis

All statistical evaluations were performed in the SPSS version 15.0 (SPSS for Windows; SPSS Inc., Chicago, IL, United States). Results of qRT-PCR analyses, histomorphometric analysis and IHC OD score analysis were statistically processed and mean values were calculated for all samples. Mean values are shown with standard deviation (SD). After calculating mean values ± SD, Kruskal-Wallis nonparametric ANOVA test for the determination of statistical significance was conducted. Post hoc Mann-Whitney test was used for the determination of statistically significant differences between examined groups at the same observation points. Differences were considered significant at $P < 0.05$.

RESULTS

Gene expression analysis in cells

Relative expression of endothelial-related genes (*Vwf*, *Egr1*, *Flt1* and *Vcam1*) in

uninduced ASCs at the 12th day after the P03 was upregulated compared to the expression of the same genes in the calibrator sample (P03-1d cells) (Figure 1).

Gene expression analysis in implants

Relative expression levels of four endothelial-related genes and one bone-related gene in the BC, BPUI and BPEO implant groups were determined in implants extracted at 1, 2, 4 and 8 wk after implantation and compared to the expression of the same genes in P03-1d cells combined with PRP (calibrator sample) (Figure 2). Because all animals have survived until the end of the determined *in vivo* experimental periods, there were twenty-four samples for gene expression analysis per each group (n = 24). Number of sacrificed mice per experimental period per group was six. Therefore, there were six samples (n = 6) per group per experimental period [n (BC) = 6, n (BPUI) = 6, n (BPEO) = 6] for gene expression analysis. For each examined gene expression, results were presented as mean value ± SD (Figure 2). Differences in relative genes expression between examined groups at the same observation points were considered significant at $P < 0.05$ (Figure 2).

Downregulation of *Vwf* gene expression was registered in all types of implants at each observation point (Figure 2A). In 1-week-old implants, *Vwf* gene expression was higher ($^{c}P < 0.05$) in BPEO in comparison with BPUI implants (Figure 2A). Among 4-week-old implants, BPEO had higher *Vwf* gene expression compared to BC ($^{b}P < 0.05$) and BPUI ($^{c}P < 0.05$) implants (Figure 2A). At 2 and 8 wk after implantation, BPUI implants had higher *Vwf* gene expression compared to the BC ($^{a}P < 0.05$) and BPEO ($^{c}P < 0.05$) type of implants (Figure 2A).

Upregulation of *Egr1* (Figure 2B) and *Flt1* (Figure 2C) gene expression was estimated in all examined types of implants, but gene expression profiles for these two genes were different. In 1-week-old and 2-week-old implants, *Egr1* gene expression (Figure 2B) was higher in BPUI implants compared to BC ($^{a}P < 0.05$) and BPEO ($^{c}P < 0.05$) implants. At 4 wk after implantations, the highest *Egr1* gene expression was estimated in BC implants, which was higher ($^{b}P < 0.05$) compared to BPEO implants. In 8-week-old implants, *Egr1* gene expression was higher in BPEO implants in comparison with the other two types of implants ($^{b}P < 0.05$ and $^{c}P < 0.05$).

In 1-week-old, 2-week-old and 4-week-old implants, *Flt1* gene expression was higher ($^{a}P < 0.05$) in BPUI compared to BC implants (Figure 2C). In 1-week-old implants, *Flt1* gene expression was higher ($^{c}P < 0.05$) in BPUI compared to BPEO and in BC compared to BPEO ($^{b}P < 0.05$) implants (Figure 2C). Almost the same *Flt1* gene expression level was found in 4-week-old BPUI and BPEO implants (Figure 2C). In 8-week-old implants, *Flt1* gene expression in BPUI implants decreased so that all types of implants had similar *Flt1* gene expression levels (Figure 2C).

The expression of the *Vcam1* gene was higher ($P < 0.05$) in BPUI compared to BPEO and BC at almost every observation point throughout the entire experimental period (Figure 2D). Interestingly, *Vcam1* gene expression was higher ($^{b}P < 0.05$) in BC compared to BPEO implants in 1-week-old and 8-week-old implants (Figure 2D).

The *Spp1* gene expression was lower in BC implants compared to BPUI and BPEO implants during the entire experimental period (Figure 2E). The *Spp1* gene expression was higher ($^{a}P < 0.05$) in BPUI compared to BC implants at each single observation point, and higher ($^{c}P < 0.05$) in BPUI compared to BPEO implants at the first three observation points (Figure 2E). In 2-week-old implants, *Spp1* gene expression was higher ($^{b}P < 0.05$) in BPEO than in BC implants (Figure 2E).

Histology and histomorphometry

Multinucleated giant cells (MNGCs) were rare and located onto or between BMM granules in 2-week-old BC type of implants. Loose connective tissue composed of weave-like collagen bundles, fibroblast-like and polymorphonuclear cells and blood vessels were seen between BMM granules (Figures 3A and 4A). Numerous MNGCs were noticed on and between BMM granules in 8-week-old BC implants (Figures 3D and 4D). Blood vessels (Figure 3D) and hemorrhagic fields (Figure 4D) were seen between BMM granules and at the areas of resorbed BMM (Figures 3D and 4D). Collagen fibers were well-organized near the granules, but in the spaces more distant from the granules, these fibers were still weave-like (Figure 4D). Cellularity of BC implants was good, but slightly weaker than at the previous observation point (Figures 3D and 4D). Also, bone-lining, osteoblast-like cells were seen at some places (Figure 3D).

Two-week-old BPUI implants had rare MNGCs (Figure 4B), and signs of BMM granules were seen (Figure 3B). Loose connective tissue was composed of weave-like collagen, various types of cells and hemorrhagic fields (Figure 4B). Regular connective tissue was seen next to BMM granules (Figure 4B). At the 8-wk observation point,

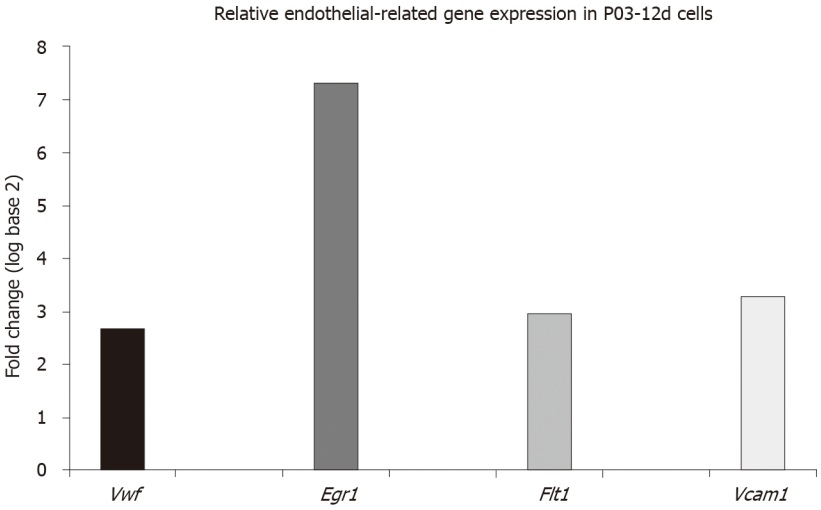

Figure 1 Relative endothelial-related gene expression in uninduced adipose-derived stem cells. Relative endothelial-related gene expression in uninduced adipose-derived stem cells at the 12th day after the third passage (P03-12d cells) compared to uninduced adipose-derived stem cells obtained 1 d after the third passage (P03-1d cells; calibrator sample). Upregulation of expression of all examined endothelial-related genes (*Vwf*, *Egr1*, *Flt1* and *Vcam1*) was found in P03-12d cells. *Vwf*: Von Willebrand factor; *Egr1*: Early growth response 1; *Flt1*: Vascular endothelial growth factor receptor 1; *Vcam1*: Vascular cell adhesion molecule 1.

MNGCs were placed onto or into BMM granules (Figures 3E and 4E) thus invading and resorbing them, while osteoblast-like cells that adhered onto BMM granules were seen only sporadically (Figure 3E). At some places, osteon-like structures invaded BMM granules (Figure 3E). Connective tissue consisted of rare blood vessels (Figure 3E), both well-organized and weave-like collagen fibers (Figure 4E).

In 2-week-old BPEO implants, BMM granules were surrounded with MNGCs, and the signs of BMM granule resorption were pronounced (Figures 3C and 4C). Collagen fibers around BMM granules and in the places more distant from the granules were mostly regular (Figure 4C). This regular connective tissue was comprised of fibroblast-like and polymorphonuclear cells, blood vessels (Figures 3C and 4C) and hemorrhagic fields (Figure 3C). Osteoblast-like cells lined and attached BMM granules and osteon-like structures invaded the granules at some places (Figure 3C). In 8-week-old BPEO implants, osteoclast-like cells (Figures 3F and 4F) and signs of BMM granules resorption (Figure 3F) were seen. Tissue between the granules had moderate vascularization (Figures 3F and 4F), well organized collagen fibers (Figure 5F) and moderate cellularity (Figure 4F). On the surface of BMM granules, osteoblast-like cells and lining cells were noticed (Figures 3F and 4F). Also, tissue regression between BMM granules was noticed (Figure 3G).

The percentage of vascularization in the BC, BPUI and BPEO groups was determined in implants extracted 2 and 8 wk after implantation. Four samples (n = 4) per each group per experimental period [n (BC) = 4, n (BPUI) = 4, n (BPEO) = 4] were taken for this analysis. For each group for both experimental periods, results were presented as mean value ± SD (Figure 5).

Among the examined types of implants, BC implants had the highest percentage of vascularization at both observation points (Figure 5). At 2 wk, those differences were significant between BC and BPUI ($^{d}P < 0.01$) and between BC and BPEO group ($^{e}P < 0.01$) (Figure 5A). Also, at this observation point BPEO implants had a higher percentage of vascularization ($^{t}P < 0.05$) in comparison with BPUI implants. In implants extracted after 8 wk (Figure 5B), differences in the percentage of vascularization was significant between BC and BPUI ($^{d}P < 0.01$) as well as between BC and BPEO implants ($^{g}P < 0.05$).

Immunohistochemical analysis

VEGFR-2 immunoexpression: VEGFR-2 immunoexpression was detected in all examined types of implants at the 2-wk and 8-wk observation point (Figure 6). VEGFR-2 immunoexpression in 2-week-old BC implants was localized in the tissue distributed between BMM granules and close to the BMM granules (Figure 6A). In 2-week-old BPUI implants, immunoexpression of VEGFR-2 was seen mostly next to the BMM granules (Figure 6B). Two weeks after implantation, BPEO implants had VEGFR-2 positive cells between BMM granules, next to the BMM granules and around

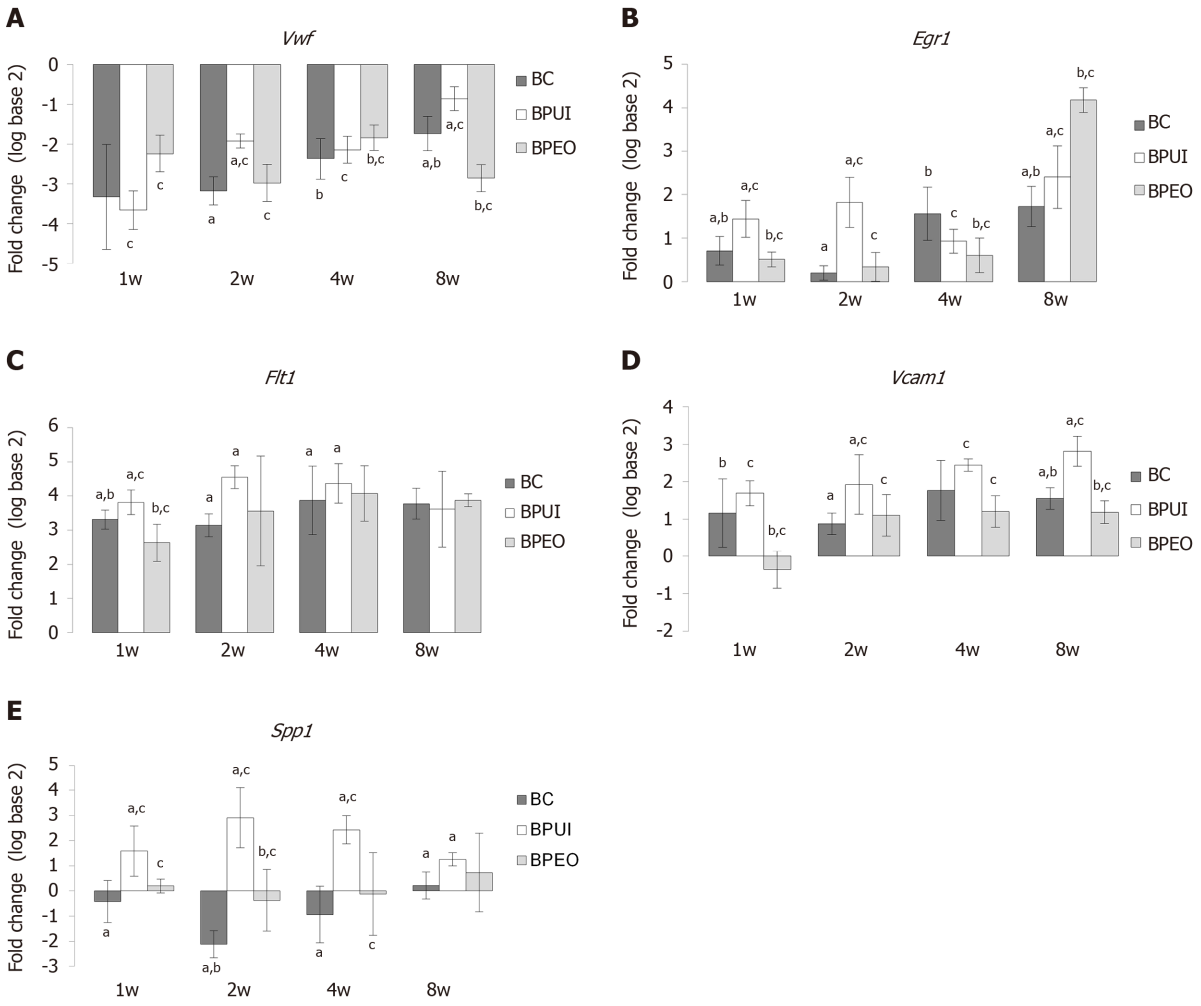

Figure 2 Dynamics and patterns of relative gene expression levels in ectopic osteogenic implants. Relative gene expression levels in BC (implants containing only BMM carrier), BPUI (implants containing uninduced adipose-derived stem cells) and BPEO (implants containing simultaneously applied endothelial and osteogenic differentiated adipose-derived stem cells) implants extracted at one (1w), two (2w), four (4w) and eight (8w) weeks after implantation (observation points) were presented comparing the expression of the same genes in the calibrator sample (P03-1d cells combined with PRP). A: Von Willebrand factor; B: Early growth response 1; C: Vascular endothelial growth factor receptor 1; D: Vascular cell adhesion molecule 1; E: Osteopontin. Number of sacrificed mice per experimental period (1w, 2w, 4w, 8w) per group was six, giving six samples per group [*n* (BC) = 6, *n* (BPUI) = 6, *n* (BPEO) = 6] for relative gene expression analysis. For each examined gene expression, results were presented as mean value ± standard deviation. Error bars represent standard deviation. $^{a}P < 0.05$ BC *vs* BPUI within the same observation point. $^{b}P < 0.05$ BC *vs* BPEO within the same observation point. $^{c}P < 0.05$ BPUI *vs* BPEO within the same observation point. *Vwf*: Von Willebrand factor; *Egr1*: Early growth response 1; *Flt1*: Vascular endothelial growth factor receptor 1; *Vcam1*: Vascular cell adhesion molecule 1; *Spp1*: Osteopontin; BC: Implants containing only bone mineral matrix carrier; BPUI: Implants containing uninduced adipose-derived stem cells, platelet-rich plasma and bone mineral matrix carrier; BPEO: Implants containing simultaneously applied endothelial and osteogenic differentiated adipose-derived stem cells, platelet-rich plasma and bone mineral matrix carrier.

blood vessels (Figure 6C). The analysis of IHC OD score revealed that, among the implants extracted 2 wk after implantation, BPUI implants had the highest VEGFR-2 IHC OD score (Figure 6G), which was higher compared to the BC ($^{a}P < 0.01$) and BPEO ($^{c}P < 0.001$) implants.

VEGFR-2 immunoexpression, distributed mainly in cells located next to the BMM granules was seen in BC implants after 8 wk (Figure 6D). At the same observation point in BPUI implants, VEGFR-2 immunoexpression was observed next to the BMM granules and in the tissue between them (Figure 6E). At the 8-wk observation point, VEGFR-2 immunoexpression in BPEO implants was similar to the expression observed in the 2-wk BPEO implants (Figure 6C and 6F), which was confirmed by IHC OD score analysis (Figure 6G). At this observation point, BPUI implants had higher VEGFR-2 immunoexpression in comparison with BPEO implants ($^{d}P < 0.001$) (Figure 6G).

CD31 immunoexpression: At the 2-wk observation point, CD31 immunoexpression in BPEO implants was stronger compared to BC ($^{b}P < 0.001$) and BPUI ($^{d}P < 0.01$) implants (Figure 7A-7A and 7G). CD31 immunoexpression was weak in BPUI implants but slightly more pronounced in 2-week-old compared to 8-week-old

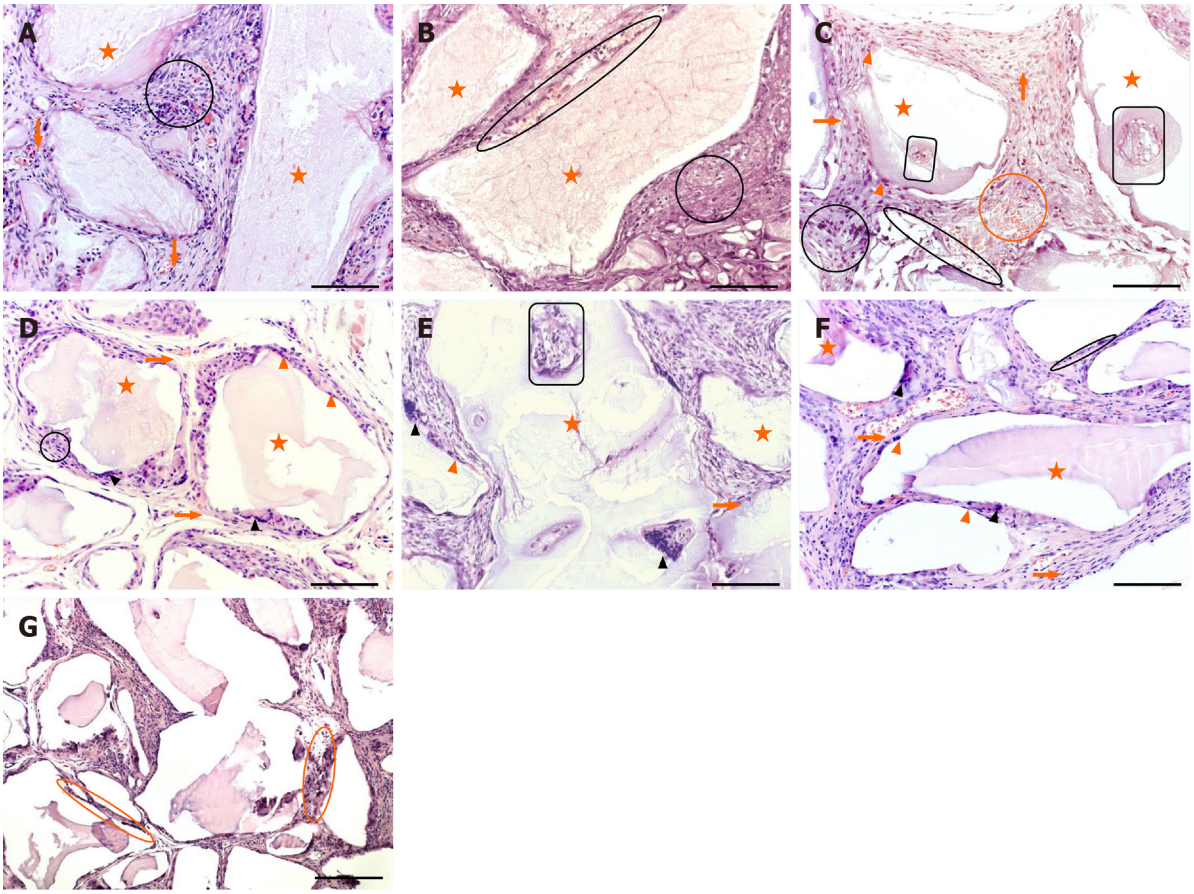

Figure 3 Representative hematoxylin and eosin sections of ectopic osteogenic implants. Representative hematoxylin and eosin sections of: A: Two-week-old BC [implants containing only bone mineral matrix (BMM) carrier]; B: Two-week-old BPUI (implants containing uninduced adipose-derived stem cells, platelet-rich plasma and BMM carrier); C: Two-week-old BPEO (implants containing simultaneously applied endothelial and osteogenic differentiated adipose-derived stem cells, platelet-rich plasma and BMM carrier); D: Eight-week-old BC implants; E: Eight-week-old BPUI implants; F and G: Eight-week-old BPEO implants. All images acquired at bright field. Scale bars show 50 μm (A-F) and 100 μm (G). BMM granules (orange star), cellularity (black circle), blood vessels (orange arrows), osteoblast-like cells (orange arrowhead), multinucleated giant cells (black arrowhead), osteon-like structures (rounded rectangle), hemorrhagic fields (orange circle), area of resorbed granules (ellipse), tissue regression between BMM granules (orange ellipse).

implants (Figure 7B and 7E). CD31 was immunoexpressed in blood vessel walls and in the tissue distributed between BMM granules in the BPEO implants at 2 wk. (Figure 7C). In the BPEO implants extracted after 8 wk, CD31 was mostly immunoexpressed in blood vessel walls (Figure 7F). Eight weeks after implantation, the IHC OD score was higher in BPEO in comparison with the BC ($^{c}P < 0.05$) and the BPUI ($^{e}P < 0.001$) group (Figure 7G).

Osteocalcin immunoexpression: Osteocalcin immunoexpression in BC implants after 2 wk was found in the space between the BMM granules (Figure 8A). It had similar distribution but lower ($^{f}P < 0.01$) IHC OD score at the 8-wk observation point in comparison with the previous observation point (Figures 8A, 8D and 8G). In BPUI implants, osteocalcin immunoexpression was seen at both observation points (Figure 8B and 8E), but it was weaker in 2-week-old (Figure 8E) compared to 8-week-old implants (Figure 8B), which was verified by the IHC OD score ($^{g}P < 0.001$) (Figure 8G). In 2-week-old BPEO implants, most of the tissue between BMM granules was osteocalcin positive (Figure 8C). In 8-week-old BPEO implants, the distribution pattern of osteocalcin immunoexpression was the same as in 2-week-old (Figure 8C and 8F), but the IHC OD score showed an increase in the intensity of osteocalcin immuno- expression (Figure 8G). Statistical significance in osteocalcin immuno-expression was shown between all examined types of implants and at both observation points except between BC and BPEO implants at the 2-wk observation point (Figure 8G).

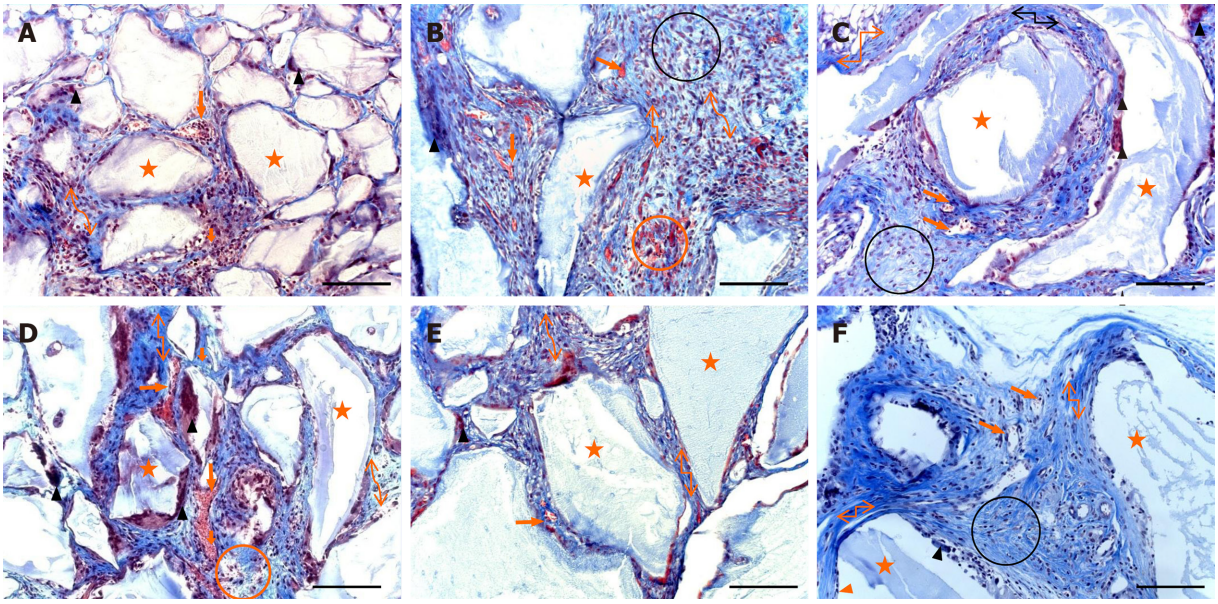

Figure 4 Representative Masson's trichrome sections of ectopic osteogenic implants. Representative Masson's trichrome sections of: A: Two-week-old BC [implants containing only bone mineral matrix (BMM) carrier]; B: Two-week-old BPUI (implants containing uninduced adipose-derived stem cells, platelet-rich plasma and BMM carrier); C: Two-week-old BPEO (implants containing simultaneously applied endothelial and osteogenic differentiated adipose-derived stem cells, platelet-rich plasma and BMM carrier); D: Eight-week-old BC implants; E: Eight-week-old BPUI implants; F: Eight-week-old BPEO implants. All images acquired at bright field. Scale bar shows 50 μm; BMM granules (orange star), cellularity (black circle), blood vessels (orange arrows), osteoblast-like cells (orange arrowhead), multinucleated giant cells (black arrowhead), hemorrhagic fields (orange circle), weave-like collagen fibers (curved double-arrow connector), regular collagen fibers (elbow double-arrow connector).

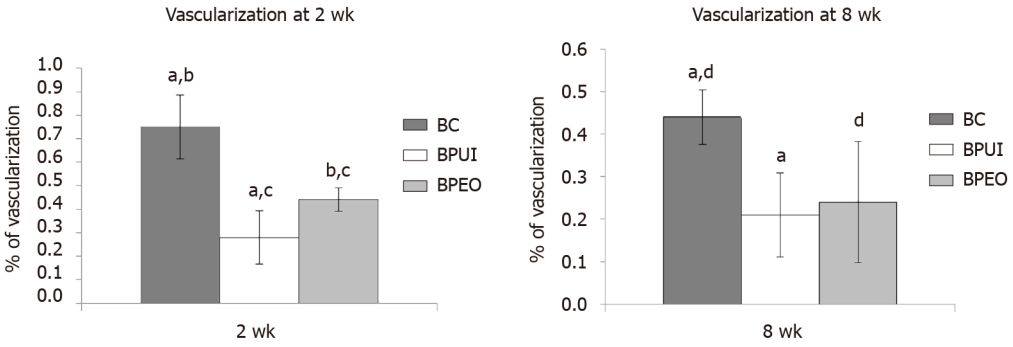

Figure 5 Histomorphometric analysis of ectopic osteogenic implants. Percentage of vascularization was determined in: A: Two-week-old and B: Eight-week-old BC [implants containing only bone mineral matrix (BMM) carrier], BPUI (implants containing uninduced adipose-derived stem cells, platelet-rich plasma and BMM carrier) and BPEO (implants containing simultaneously applied endothelial and osteogenic differentiated adipose-derived stem cells, platelet-rich plasma and BMM carrier). Four samples (n = 4) per each group per experimental period [n (BC) = 4, n (BPUI) = 4, n (BPEO) = 4] were taken for this analysis. For each group for both experimental periods, results were presented as mean values ± standard deviation. Error bars represent standard deviation. $^{a}P < 0.01$ BC *vs* BPUI. $^{b}P < 0.01$ BC *vs* BPEO. $^{c}P < 0.05$ BPUI *vs* BPEO. $^{d}P < 0.05$ BC and BPEO. BC: Implants containing only bone mineral matrix carrier; BPUI: Implants containing uninduced adipose-derived stem cells, platelet-rich plasma and bone mineral matrix carrier; BPEO: Implants containing simultaneously applied endothelial and osteogenic differentiated adipose-derived stem cells, platelet-rich plasma and bone mineral matrix carrier.

DISCUSSION

In uninduced ASCs, examined endothelial-related genes, *Vwf, Egr1, Flt1* and *Vcam1*, were upregulated 12 d after the P03 compared to the calibrator sample (P03-1d cells). Vasculogenic potential of uninduced ASCs could be attributed to the fact that upon isolation and transfer to a culture dish, MSCs may proceed to differentiate in accordance with the culture conditions[37] or by the influence of growth factors contained within FBS[38].

Relative expression levels of endothelial-related genes in implants were generally higher in BPUI compared to BC and BPEO implants. One of the reasons for such an expression pattern in BPUI implants was probably the presence of biological factors released upon PRP activation because these factors accelerate and improve ASC *in vivo* differentiation[29,39,40]. One of those growth factors is platelet-derived growth factor,

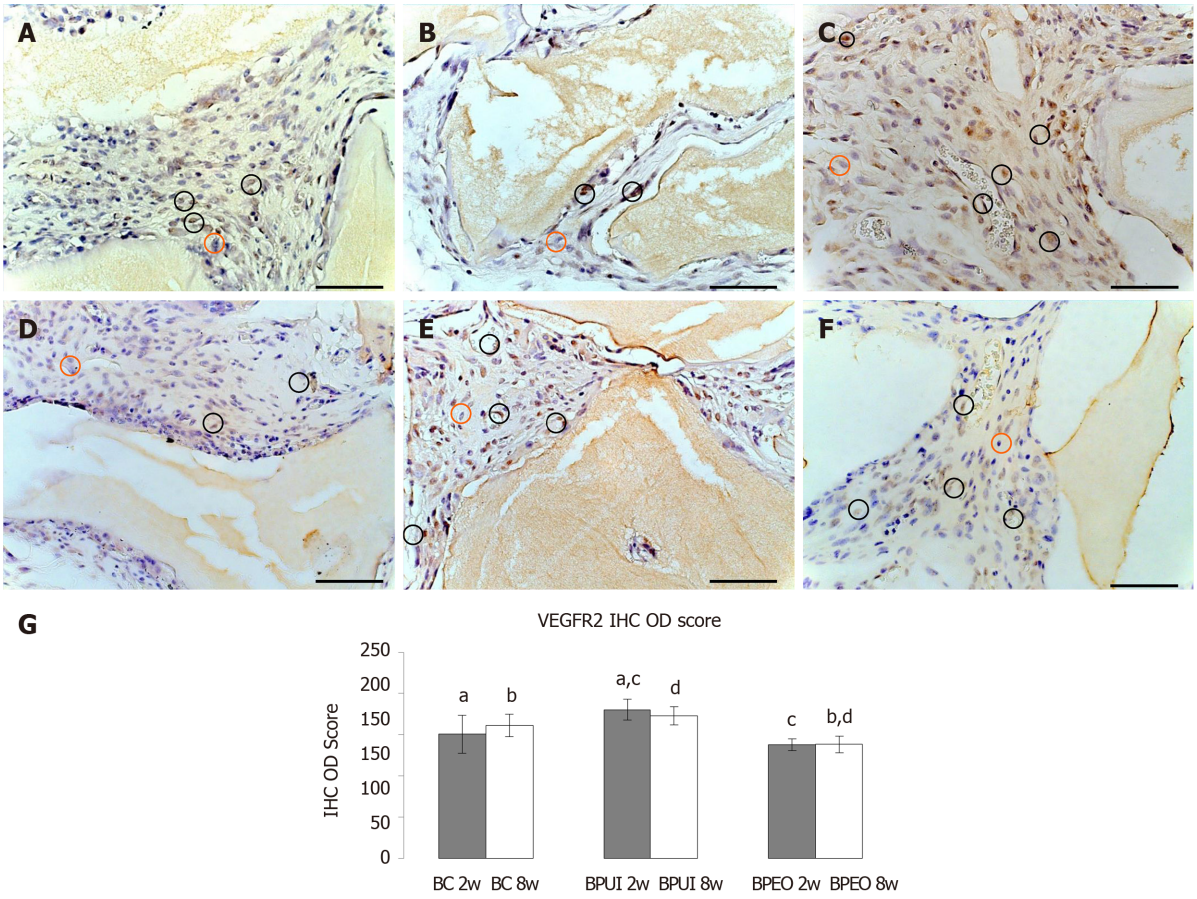

Figure 6 Immunoexpression of vascular endothelial growth factor receptor 2 in representative sections of ectopic osteogenic implants. A: Two-week-old BC [implants containing only bone mineral matrix (BMM) carrier]; B: Two-week-old BPUI (implants containing uninduced adipose-derived stem cells, platelet-rich plasma and BMM carrier); C: Two-week-old BPEO (implants containing simultaneously applied endothelial and osteogenic differentiated adipose-derived stem cells, platelet-rich plasma and BMM carrier); D: Eight-week-old BC implants; E: Eight-week-old BPUI implants; F: Eight-week-old BPEO implants, G: Vascular endothelial growth factor receptor 2 immunohistochemistry optical density score in implants extracted two (2w) and eight (8w) weeks after implantation (observation points). All images acquired at bright field. Scale bar shows 20 μm. Immunoreactivity is visualized as brown color and represents immunoexpression of the applied antibody. Vascular endothelial growth factor receptor-2 positive cell (black circle); Vascular endothelial growth factor receptor-2 negative cell (orange circle). [a]*P* < 0.01 BC 2w *vs* BPUI 2w. [b]*P* < 0.001 BC 8w *vs* BPEO 8w. [c]*P* < 0.001 BPUI 2w *vs* BPEO 2w. [d]*P* < 0.001 BPUI 8w *vs* BPEO 8w. VEGFR-2: Vascular endothelial growth factor receptor 2; BC: Implants containing only bone mineral matrix carrier; BPUI: Implants containing uninduced adipose-derived stem cells, platelet-rich plasma and bone mineral matrix carrier; BPEO: Implants containing simultaneously applied endothelial and osteogenic differentiated adipose-derived stem cells, platelet-rich plasma and bone mineral matrix carrier; IHC: Immunohistochemistry; OD: Optical density.

which induces angiogenesis both indirectly and directly. Indirect influence is reflected in enhancing VEGF secretion that further leads to EC migration and vascular tubule formation[41,42]. Directly, platelet-derived growth factor induces endothelial differentiation of stem cells *via* the Akt signaling pathway[43].

Additionally, uninduced cells that are components of the BPUI implants had upregulated expression of endothelial-related genes prior to implantation. *Egr1*, activated by angiopoetin-1 *via* the Erk1/2, PI-3 kinase/AKT and mTOR signaling pathway, can be upregulated in response to growth factors, cytokines or hypoxia[44] in various types of cells including ECs, smooth muscle cells, fibroblasts and leukocytes[45]. The highest fold change in *Egr1* gene expression was estimated in BPEO implants at the 8-wk observation point compared to the 4-wk observation point. The transcription factor that controls *Flt1*[46] and *Vcam1*[47] gene expression is encoded by *Egr1*. Therefore, the increase in the expression of these two genes in BPEO implants at later observation points could be explained by later onset of *Egr1* gene expression.

Expression of *Flt1* was the highest at the 2-wk observation point in BPUI implants and at the 4-wk observation point in BC and BPEO implants. The *Flt1* gene encodes VEGFR-1, a protein responsible for recruitment of EC progenitors[48], but it is also expressed on monocytes and macrophages thus regulating their migration[49,50]. Therefore, *Flt1* gene expression in our implants could be related to ECs and their progenitors as well as monocytes and macrophages.

Vcam1 gene expression was the highest at the 4-wk observation point in BC and BPEO implants and in BPUI implants at the 8-wk observation point. At each

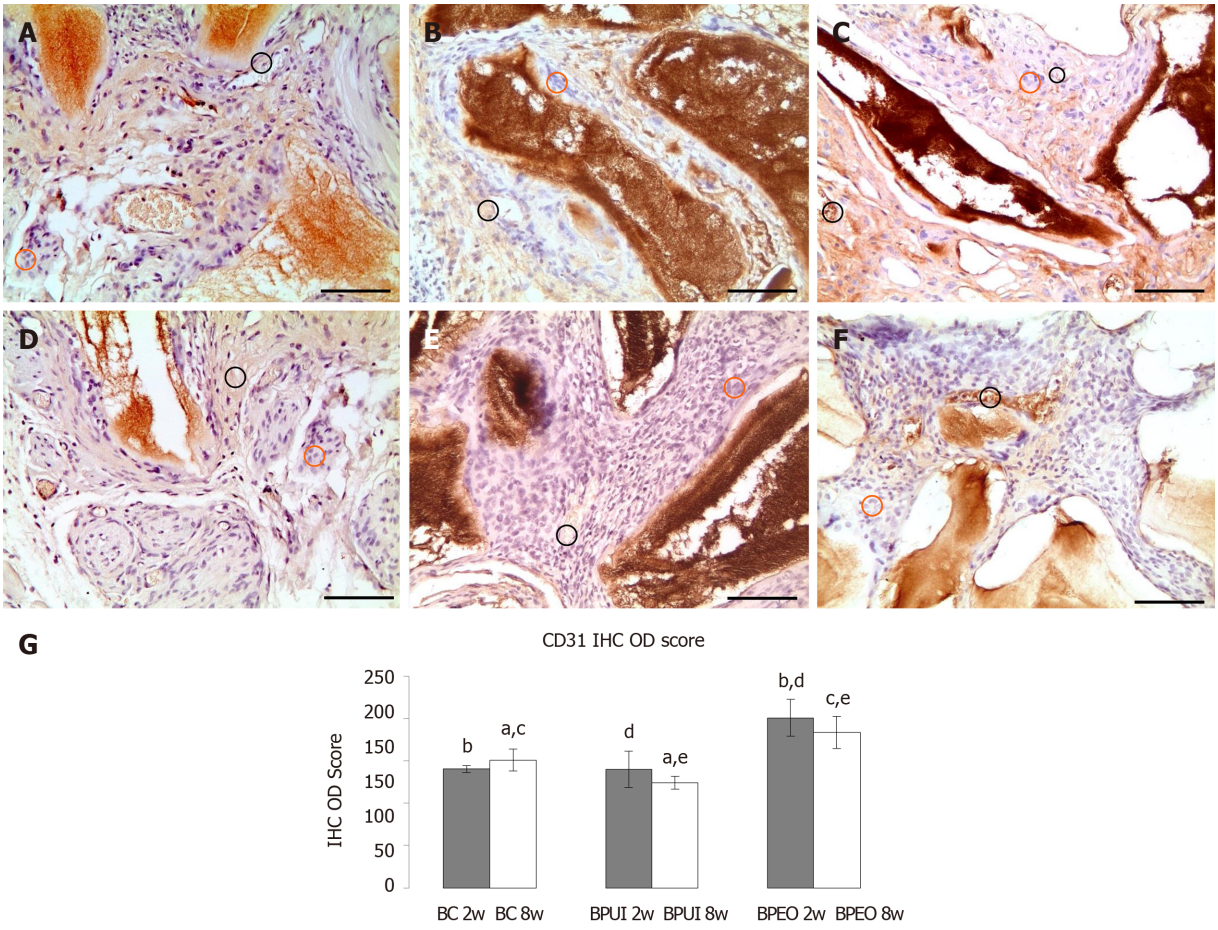

Figure 7 Immunoexpression of CD31 in representative sections of ectopic osteogenic implants. A: Two-week-old BC [implants containing only bone mineral matrix (BMM) carrier]; B: Two-week-old BPUI (implants containing uninduced adipose-derived stem cells, platelet-rich plasma and BMM carrier); C: Two-week-old BPEO (implants containing simultaneously applied endothelial and osteogenic differentiated adipose-derived stem cells, platelet-rich plasma and BMM carrier); D: Eight-week-old BC implants; E: Eight-week-old BPUI implants; F: Eight-week-old BPEO implants; G: CD31 immunohistochemistry optical density score in implants extracted two (2w) and eight (8w) weeks after implantation (observation points). All images acquired at bright field. Scale bar shows 50 μm. Immunoreactivity is visualized as brown color and represents immunoexpression of the applied antibody. CD31 positive cells (black circle), CD31 negative cells (orange circle). $^{a}P < 0.01$; BC 8w *vs* BPUI 8w. $^{b}P < 0.001$; BC 2w *vs* BPEO2w. $^{c}P < 0.05$; BC 8w *vs* BPEO 8w. $^{d}P < 0.01$; BPUI 2w *vs* BPEO 2w. $^{e}P < 0.001$; BPUI 8w *vs* BPEO 8w. BC: Implants containing only bone mineral matrix carrier; BPUI: Implants containing uninduced adipose-derived stem cells, platelet-rich plasma and bone mineral matrix carrier; BPEO: Implants containing simultaneously applied endothelial and osteogenic differentiated adipose-derived stem cells, platelet-rich plasma and bone mineral matrix carrier; IHC: Immunohistochemistry; OD: Optical density.

observation point, *Vcam1* expression was the highest in BPUI implants. Its expression can be contributed to ECs that express *Vcam1* after stimulation by cytokines thus mediating adhesion of lymphocytes or monocytes to the vascular endothelium[51] but also with stromal cells that express this gene during the interaction with its corresponding ligand on osteoclast precursors[52] and pericytes[53].

The expression of *Vwf* in BPEO implants was the highest at the 4-wk observation point, while in BC and BPUI implants, the expression peak of this gene was estimated at the 8-wk observation point. These results are not surprising because *Vwf* is expressed in late angiogenesis[54]. *Vwf* encodes large plasma glycoprotein mainly expressed in vascular ECs[55]. Besides ECs, this expression could be attributed to megakaryocytes and platelets[56].

Among the examined groups, the IHC OD score for VEGFR-2 was the highest in BPUI implants at both observation points, which was statistically significant. VEGFR-2 is highly expressed on EC progenitors in early embryogenesis but later decreases[57], which is reflected in the VEGFR-2 immunoexpression pattern in the BPUI implants. High VEGFR-2 immunoexpression in BPUI implants is most likely related to the presence of numerous EC progenitors and not with well-developed blood vessels because the percentage of vascularization was low in this implant. VEGFR-2 is a tyrosine kinase type receptor for VEGF isoform A (VEGF-A). VEGF-A/VEGFR-2 is the most notable ligand-receptor complex within the VEGF system[58]. Specifically, binding of VEGF-A to VEGFR-2 phosphorylates tyrosine residues and activates VEGFR-2, which further regulates angiogenesis and EC functions[59]. Through such action on ECs,

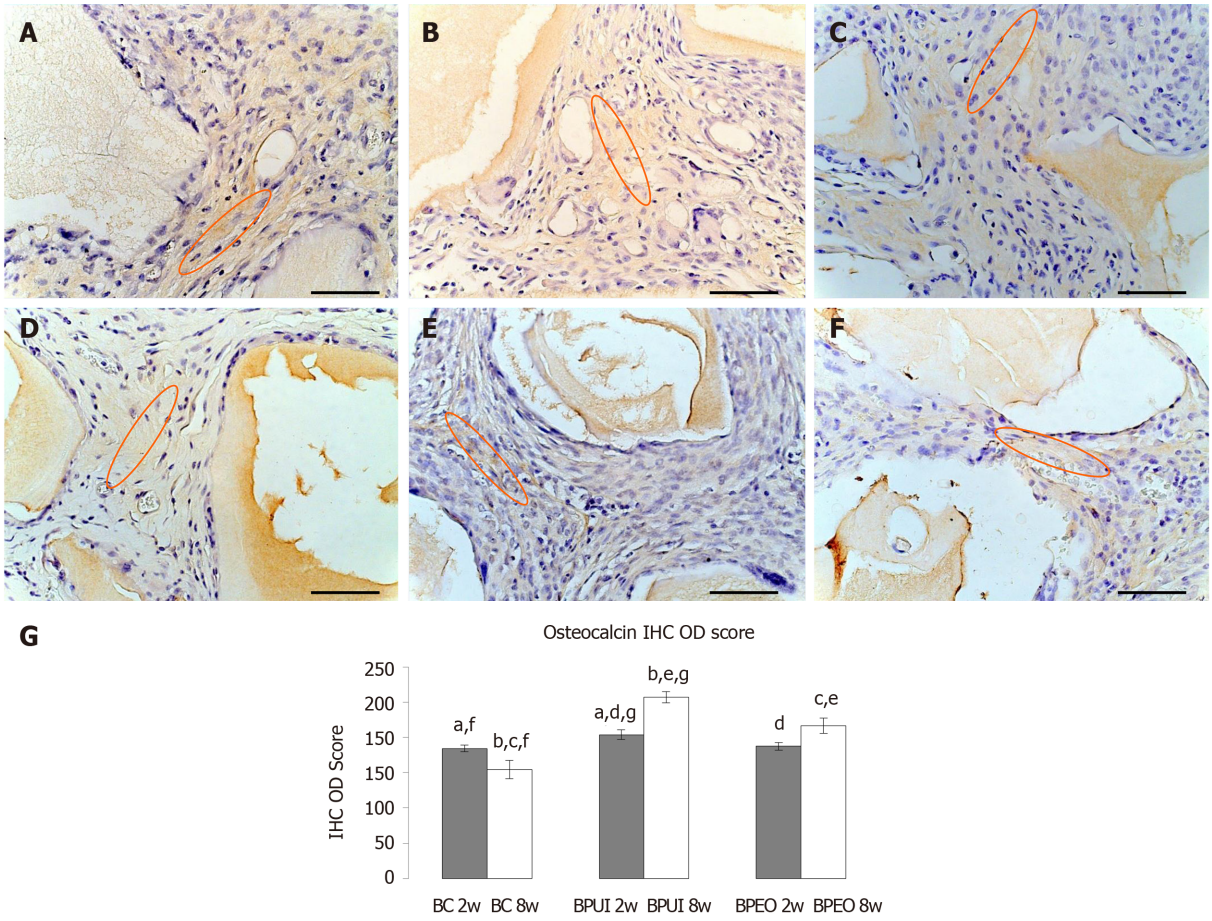

Figure 8 Immunoexpression of osteocalcin in representative sections of ectopic osteogenic implants. A: Two-week-old BC [implants containing only bone mineral matrix (BMM) carrier]; B: Two-week-old BPUI (implants containing uninduced adipose-derived stem cells, platelet-rich plasma and BMM carrier]; C: Two-week-old BPEO (implants containing simultaneously applied endothelial and osteogenic differentiated adipose-derived stem cells, platelet-rich plasma and BMM carrier); D: Eight-week-old BC implants; E: Eight-week-old BPUI implants; F: Eight-week-old BPEO implants; G: Osteocalcin immunohistochemistry optical density score in implants extracted two (2w) and eight (8w) weeks after implantation (observation points). All images acquired at bright field. Scale bar shows 20 μm. Immunoreactivity is visualized as brown color and represents immunoexpression of the applied antibody; osteocalcin-positive fields (orange ellipse). [a]*P* < 0.01; BC 2w *vs* BPUI2w. [b]*P* < 0.001; BC 8w *vs* BPUI 8w. [c]*P* < 0.001; BC 8w *vs* BPEO 8w. [d]*P* < 0.05; BPUI 2w *vs* BPEO 2w. [e]*P* < 0.001; BPUI 8w *vs* BPEO 8w. [f]*P* < 0.01; BC 2w *vs* BC8w. [g]*P* < 0.001; BPUI 2w *vs* BPUI 8w. BC: Implants containing only bone mineral matrix carrier; BPUI: Implants containing uninduced adipose-derived stem cells, platelet-rich plasma and bone mineral matrix carrier; BPEO: Implants containing simultaneously applied endothelial and osteogenic differentiated adipose-derived stem cells, platelet-rich plasma and bone mineral matrix carrier; IHC: Immunohistochemistry; OD: Optical density.

which increases blood vessel density, VEGF consequently increases osteogenesis[60,61]. In addition, VEGFRs are also expressed on MSCs, OBs and osteoclasts, so VEGF can directly bind to osteoprogenitor MSCs[62], OBs[63] and osteoclasts[64]. The results of those VEGF-VEGFRs interactions can be enhanced by mineralization in osteoprogenitor cells[62], increased activity of alkaline phosphatase[65] and enhanced capability of migration and differentiation of OBs[63].

CD31 is an adhesion protein responsible for vascular permeability, coagulation and transmigration of inflammatory cells[66]. At the 2-wk observation point, the IHC OD score for CD31 was statistically higher in BPEO compared to BC and BPUI implants. This indicates the existence of large numbers of junctions between adjacent ECs in BPEO implants because this protein is highly expressed at these junctions[67]. However, a slight decrease in the IHC OD score for CD31 was estimated at the 8-wk observation point compared to the 2-wk observation point in BPEO implants. It may indicate that initially strong stimulation of vascularization achieved by simultaneous application of ECs and OBs in this type of implant decreases during a longer experimental period. However, the IHC OD score for CD31 at 8-wk was still significantly higher in BPEO implants in comparison with the other two groups. Besides being the most sensitive pan-endothelial marker expressed on numerous microvessels[68] and on single endothelial progenitor[69] or mature ECs[69,70], CD31 can also be expressed on leukocytes, some hematopoietic cells and platelets[66,70]. These findings could explain how BPUI implants possess CD31 immunoexpression and a low percentage of vascularization at the same time.

At first glance, some results of gene expression and the IHC OD score analysis seemed contradictory compared to histomorphometric analysis. Specifically, the percentage of vascularization was higher in the BC group compared to the other two groups at both observation points and higher in the BPEO than in the BPUI group at both observation points. This discrepancy can be explained by two facts. First, histomorphometric measurements were done only on those blood vessels with the histological characteristics of the blood vessel, whereas endothelial-related genes and proteins are expressed in blood vessel cells and in EC progenitors and in a few other types of cells (mentioned above). Second, some tissue sections had hemorrhagic fields that were not included in histomorphometric measurements, but they can contribute to higher endothelial-related gene expression.

At the 2-wk observation point, resorption of BMM granules was more pronounced in BPEO than in the two other types of implants, which could be in relation with MNGCs that were the most abundant in this group. As a consequence in BPEO implants, signs of intensive resorption of BMM granules at the 8-wk observation point could be seen. In BC and BPUI implants MNGCs were more abundant and signs of BMM granule resorption were more advanced at 8-wk compared to the previous observation point but still weaker than in BPEO implants. Although regular collagen fibers replaced weave-like collagen fibers at the 8-wk observation point and osteoblast-like cells were seen at some places, mineralization of the tissue that had osteoid-like appearance in BC implants was poor, which was indicated by osteocalcin immunoexpression. Osteoblast-like cells in BC implants are probably differentiated from resident MSCs that are recruited in an intramembranous pathway induced by implanted biomaterial[71]. Namely, BC implants had only Bio-Oss™, a calcium-phosphate (CP)-based biomaterial in their composition. CP-based biomaterials elicit an inflammatory response upon implantation that attracts the infiltration of resident mono- and multinucleated cells and subsequently activates osteoclastogenesis[72], which results in CP degradation and resorption[73]. Released Ca^{2+} and PO_4^{3-} stimulate osteoprogenitor cell differentiation and bone matrix deposition[74]. Presence of osteoblast-like cells and significantly higher IHC OD score for osteocalcin in BPUI implants in comparison with BC and BPEO implants could be attributed to the effect elicited by combination of PRP and uninduced ASCs in the composition of these implants, which is in accordance with the synergistic effect earlier observed between these two components[75]. Regardless of the application of the source of growth factors, CP-based biomaterials can accelerate osteogenic differentiation of stem cells[55]. One of the possible underlying mechanisms is an increase in calcium ions that enhance osteogenic differentiation through the L-type calcium channel-mediated signal pathway. Also, an increase in phosphate ions accelerate the sodium-phosphate symporter that move the ions and as a consequence induce osteogenic differentiation of nonskeletal cells as well as formation of apatite[76,77]. It has also been reported that transplanted ASCs are able to differentiate into vascular ECs and OBs, which can be one more explanation for the presence of endothelial-like and osteoblast-like cells in BPUI implants[78].

Unlike BC and BPUI implants, BPEO implants had regular collagen fibers at both observation points. Osteon-like structures invaded, and cuboidal-shaped osteoblast-like cells lined and attached BMM granules in BPEO implants at the 2-wk observation point; at the 8-wk observation point some cells that lined BMM granules were still cuboidal-shaped, while others had a flattened appearance, similar to inactive OBs. BPEO implants had mild osteocalcin immunoexpression at 2-wk and strong osteocalcin immunoexpression at 8-wk, which the IHC OD score for osteocalcin confirmed. Interaction of implanted OBs and ECs in BPEO implants through few existing types of gap junctions, including Cx43, Cx37 and Cx40[79], is one of the possible explanations for the observed histological picture and osteocalcin immunoexpression within these implants. Communication *via* Cx43 gap junctions induced expression of markers of OB differentiation including osteocalcin[80], an osteogenic marker with the most selective expression pattern among the products of OBs[81]. Mature OBs produce osteocalcin that is further deposited onto extracellular matrix, which indicates bone repair[82].

The second possible mechanism that led to development of the osteogenic process in BPEO implants is crosstalk between diffusible factors released from ECs and OBs. OBs secrete VEGF and fibroblast growth factor[83]. VEGF is a powerful stimulator of EC differentiation[3,84], while fibroblast growth factor stimulates EC migration and proliferation[85]. In turn, ECs secrete bone morphogenic protein-2, endothelin-1, platelet-derived growth factor, transforming growth factors β, insulin-like growth factor, epidermal growth factor and osteoprotegerin[3,86,87] that can induce differentiation of osteoprogenitor cells into OBs or have mitogenic and/or chemotactic

effects on OBs.

At each observation point, *Spp1* gene expression was the lowest in the BC group, while it was upregulated in BPEO group at the 1-wk and 8-wk observation points. The BPUI group had higher *Spp1* gene expression than the other two groups, probably due to the ability of ASCs to secrete cytokines and chemokines that are homing signals for endogenous stem and progenitor cells to the site of injury[88]. The presence of osteopontin is critical for remodeling of the mature bone when its role is in anchorage of osteoclasts to mineralized bone matrix[89]. Along with osteocalcin, it is a marker of middle and late osteogenic process[90]. In spite of all favorable features of BPEO implants, the regression of the tissue between BMM granules was observed, which could be a sign that stimulation was too strong.

Osteocalcin immunoexpression and *Spp1* gene expression were lower in BC compared to BPUI and BPEO implants. Specifically, *Spp1* gene expression was significantly higher in BPUI compared to BC implants at each observation point and significantly higher in BPEO implants compared to BC implants at the 2-wk observation point. The IHC OD score for osteocalcin was significantly higher at both observation points in BPUI than in BC implants and significantly higher in BPEO than in BC implants at the 8-wk observation point. The existence of more intensive osteocalcin immunoexpression, higher *Spp1* gene expression and more osteoblast-like cells in the types of implants enriched with cells and PRP compared to BC implants is in accordance with one study performed on an orthotopic model[91]. On a dog mandible defect model, bone regeneration was faster and bone quality much better in the defects filled with the biological triad compared to the ones without MSCs. Maybe the key reason for the positive effect of the biological triad is that adult MSCs, fibroblasts, OBs and ECs express membrane receptors specific for growth factors that are released upon PRP activation[92]. In addition, PRP contains fibrin, fibronectin and vitronectin that act as cell adhesion molecules important for migration of ECs, fibroblasts and the cells of epithelial type[93]. Also, similarity in *Spp1* gene expression between BPUI and BPEO implants indicate that factors released out of activated PRP induce the process in which *Spp1* is expressed[94].

Two weeks after implantation, BC implants had a higher percentage of vascularization compared to BPUI and BPEO implants, while VEGFR-2 immunoexpression was similar to the one in implants enriched with cells. It was estimated that these implants initially have higher expression of endothelial-related genes than BPEO implants. Also, BC implants had mild osteocalcin immunoexpression and osteopontin gene expression. However, a problem for clinical use that would be controlled for a longer period of time is the lowering of bone-related gene and protein expression.

The expression of endothelial-related genes and IHC OD score for osteocalcin in BPUI implants compared to BC and BPEO implants was higher in almost every observation point, which was mostly significant. Regardless, the percentage of vascularization was the weakest in BPUI among the examined types of implants at both observation points ($P < 0.05$) and ($P < 0.01$). Also, there was no statistically significant change in the percentage of vascularization between the 2-wk and 8-wk observation points in the BPUI group. In addition to a low percentage of vascularization, *Spp1* gene expression decreased during the *in vivo* experimental period, which could be a drawback for translation of the approach that includes uninduced ASCs in osteogenic implants to the clinical application.

In BPEO implants, tissue regression between BMM granules is large, which could be a sign that stimulation was too strong in BPEO implants and could represent the problem for their clinical application. Too strong stimulation could be related to the 1:1 ratio of ECs/OBs. According to some studies, ECs and OBs applied in this ratio have a more favorable effect on vascularization and osteogenic process than the application of endothelial differentiated ASCs or osteogenic differentiated ASCs alone or uninduced ASCs[95] seeded into RADA16-I scaffolds. Others have reported that the same ratio of ECs/OBs did not lead to enhanced vascularization or osteogenic process in comparison with uninduced ASCs seeded on polylactic acid gas-plasma-treated scaffolds[19]. Therefore, in order to favor their beneficial effects on vascularization and osteogenic process and to avoid tissue regression, different EC/OB ratios should be further analyzed. When determining the optimal EC/OB ratio in osteogenic implants, the following considerations should be account for: (1) OBs secrete VEGF; (2) ECs secrete bone morphogenic protein-2; (3) VEGF and bone morphogenic protein-2 have a synergistic effect on bone formation and regeneration; and (4) These two molecules in an inappropriate ratio can cause adverse effect on this processes[96,97]. In addition, it was found that overexpressed VEGF can be a reason for enhanced bone tissue resorption[98].

To summarize, the percentage of vascularization was significantly higher in BC

constructs compared to BPUI and BPEO constructs 2 and 8 wk after implantation. Also, BC constructs had a mild IHC OD score for VEGFR-2. However, BC constructs had the lowest endothelial-related gene (*Vwf*, *Egr1*, *Flt1* and *Vcam1*) expression among the examined types of constructs that was followed by the weakest osteocalcin immunoexpression confirmed by the IHC OD score and mostly downregulated *Spp1* gene expression. Endothelial-related gene expression was generally higher in BPUI constructs compared to BC and BPEO constructs, which was mostly significant, but histomorphometrical analysis showed the lowest percentage of vascularization in the BPUI group. BPEO constructs had a higher percentage of vascularization compared to BPUI constructs at 2 wk and 8 wk. Endothelial-related gene expression in BPEO constructs had a later onset. However, with the exception of *Vwf*, these genes were upregulated and well-balanced through the whole *in vivo* experimental period. CD31 immunoexpression was significantly higher in BPEO implants compared to BC and BPUI implants at both observation points. The *Spp1* gene expression was higher in 8-week-old BPEO implants compared to 1-week-old, 2-week-old and 4-week-old BPEO implants. Osteocalcin immunoexpression was pronounced at eight weeks in BPEO constructs, and the IHC OD score showed that it increased in 8-week-old compared to 2-week-old BPEO implants. However, in 8-week-old BPEO constructs, strong tissue regression was observed between BMM granules.

CONCLUSION

BPEO constructs, which consist of both endothelial and osteogenic differentiated ASCs, have a favorable impact on vascularization and osteogenesis in an ectopic bone-forming model. However, tissue regression at later time points imposes the need for discovering the optimal ratio of ECs/OBs within the BPEO constructs prior to considerations for clinical applications.

ARTICLE HIGHLIGHTS

Research background

A major problem in the healing of bone defects is insufficient or absent blood supply within the defect. To overcome this challenging problem, a plethora of approaches within bone tissue engineering (BTE) have been developed recently. For successful bone tissue regeneration, osteogenesis and vasculogenesis should be supported by an appropriate combination of cells, growth factors and biomaterials, which represent the biological triad components.

Research motivation

Despite emerging developments of various approaches in the field of BTE, an optimal combination of the biological triad factors is still unknown. Bearing that in mind, our motivation was to combine endothelial differentiated and osteogenic differentiated adipose-derived stem cells (ASCs) in the same construct together with platelet-rich plasma (PRP) as a growth factor reservoir on the bone mineral matrix (BMM) as a carrier. This approach was applied in a mouse subcutaneous implantation model to examine the ectopic osteogenic potential of this type of construct, which enables interplay between endothelial cells (ECs) and osteoblasts (OBs) in induction of ectopic osteogenesis.

Research objectives

The objective of our study was to examine the effects of simultaneously applied endothelial and osteogenic differentiated ASCs combined with PRP and delivered on the BMM on vascularization and osteogenesis in ectopically implanted BTE constructs. To examine the significance of *in vitro* endothelial and osteogenic induction, BTE constructs containing uninduced ASCs, PRP and BMM were also prepared. BMM-only constructs represented a basic group of constructs that served as a carrier control.

Research methods

ASCs obtained from a stromal vascular fraction of visceral epididymal adipose tissue of BALB/c mice were cultivated up to the third passage (P03). At the P03, three types of cell cultures were established: ASCs induced into ECs, ASCs induced into OBs and

ASCs expanded *in vitro* without induction towards any cell type (uninduced ASCs). Upon cultivation and/or differentiation, three types of ectopic BTE constructs were prepared: (1) BPEO constructs: BTE constructs containing simultaneously applied endothelial and osteogenic differentiated ASCs combined with PRP and seeded onto BMM carrier; (2) BPUI constructs: BTE constructs containing uninduced ASCs, combined with PRP and seeded onto BMM carrier; and (3) BC constructs (control): BTE constructs that contained only BMM carrier. BTE constructs extracted 1, 2, 4 and 8 wk after implantation were analyzed regarding relative endothelial-related and bone-related gene expression. Histochemical, immunohistochemical and histomorphometric analyses were performed on constructs extracted 2 and 8 wk after implantation.

Research results

The percentage of vascularization was significantly higher in BC constructs compared to BPUI and BPEO after 2 and 8 wk. However, BC constructs had the lowest endothelial-related gene (*Vwf*, *Egr1*, *Flt1* and *Vcam1*) expression among the examined types of constructs. This was followed by significantly weaker osteocalcin immunoexpression in comparison with BPUI and BPEO implants and mostly downregulated *Spp1* gene expression. Endothelial-related gene expression was generally higher in BPUI constructs compared to BC and BPEO constructs, which was mostly significant. However, histomorphometric analysis showed the lowest percentage of vascularization in the BPUI group. BPEO constructs had a higher percentage of vascularization compared to BPUI constructs at 2 wk and 8 wk. Endothelial-related gene expression in BPEO constructs had a later onset, but with the exception of *Vwf*, these genes were upregulated and well-balanced through the whole *in vivo* experimental period. In addition, CD31 immunoexpression was significantly higher in BPEO compared to BC and BPUI implants at both observation points. This also led to the late onset of *Spp1* gene expression, although osteocalcin immunoexpression was pronounced at both observation points. The IHC OD score showed osteocalcin immunoexpression increased in BPEO implants at 8 wk compared to 2 wk. In BPEO constructs, tissue regression was observed between BMM granules after 8 wk.

Research conclusions

Ectopically implanted BPEO constructs have a favorable impact on vascularization and osteogenesis but observed tissue regression at later time points imposes the need for discovering the optimal ratio of ECs/OBs within the BPEO constructs prior to consideration for clinical applications.

Research perspectives

Obtained results unequivocally indicate the potential of such an approach, which could be used for further preclinical evaluations in the orthotopic model regarding optimization of EC/OB ratio within bone tissue-engineered constructs.

ACKNOWLEDGEMENTS

The authors would like to thank Radenković M for her assistance with the IHC OD score analysis in ImageJ software.

REFERENCES

1 **Derkus B**, Okesola BO, Barrett DW, D'Este M, Chowdhury TT, Eglin D, Mata A. Multicomponent hydrogels for the formation of vascularized bone-like constructs in vitro. *Acta Biomater* 2020; **109**: 82-94 [PMID: 32311533 DOI: 10.1016/j.actbio.2020.03.025]

2 **Dompe C**, Wąsiatycz G, Mozdziak PE, Jankowski M, Kempisty B. Current clinical applications of adipose-derived stem cells in humans and animals. *MJCB* 2019; **7**: 105-111 [DOI: 10.2478/acb-2019-0014]

3 **Dimitriou R**, Tsiridis E, Giannoudis PV. Current concepts of molecular aspects of bone healing. *Injury* 2005; **36**: 1392-1404 [PMID: 16102764 DOI: 10.1016/j.injury.2005.07.019]

4 **Portal-Núñez S**, Lozano D, Esbrit P. Role of angiogenesis on bone formation. *Histol Histopathol* 2012; **27**: 559-566 [PMID: 22419020 DOI: 10.14670/HH-27.559]

5 **Inomata K**, Honda M. Co-Culture of Osteoblasts and Endothelial Cells on a Microfiber Scaffold to Construct Bone-Like Tissue with Vascular Networks. *Materials (Basel)* 2019; **12** [PMID: 31491993 DOI: 10.3390/ma12182869]

6 **Rouwkema J**, Rivron NC, van Blitterswijk CA. Vascularization in tissue engineering. *Trends Biotechnol* 2008; **26**: 434-441 [PMID: 18585808 DOI: 10.1016/j.tibtech.2008.04.009]

7 **Laranjeira MS**, Fernandes MH, Monteiro FJ. Reciprocal induction of human dermal microvascular endothelial cells and human mesenchymal stem cells: time-dependent profile in a co-culture system. *Cell Prolif* 2012; **45**: 320-334 [PMID: 22607133 DOI: 10.1111/j.1365-2184.2012.00822.x]

8 **Zhou J**, Dong J. Vascularization in the Bone Repair. In: Lin Y. Osteogenesis. Rijeka, Croatia: IntechOpen, 2012: 287-296 [DOI: 10.5772/36325]

9 **Villars F**, Guillotin B, Amédée T, Dutoya S, Bordenave L, Bareille R, Amédée J. Effect of HUVEC on human osteoprogenitor cell differentiation needs heterotypic gap junction communication. *Am J Physiol Cell Physiol* 2002; **282**: C775-C785 [PMID: 11880266 DOI: 10.1152/ajpcell.00310.2001]

10 **Castro-Piedra S**, Morales-Sánchez J. Mesenchymal stem cell isolation from mice inguinal fat tissue: a protocol to get the best from small samples. *Tecnología en Marcha* 2019; **32**: 69-80 [DOI: 10.18845/tm.v32i4.4793]

11 **Najman SJ**, Cvetković VJ, Najdanović JG, Stojanović S, Vukelić-Nikolić MĐ, Vučković I, Petrović D. Ectopic osteogenic capacity of freshly isolated adipose-derived stromal vascular fraction cells supported with platelet-rich plasma: A simulation of intraoperative procedure. *J Craniomaxillofac Surg* 2016; **44**: 1750-1760 [PMID: 27624644 DOI: 10.1016/j.jcms.2016.08.011]

12 **Kokai LE**, Marra K, Rubin JP. Adipose stem cells: biology and clinical applications for tissue repair and regeneration. *Transl Res* 2014; **163**: 399-408 [PMID: 24361334 DOI: 10.1016/j.trsl.2013.11.009]

13 **Devitt SM**, Carter CM, Dierov R, Weiss S, Gersch RP, Percec I. Successful isolation of viable adipose-derived stem cells from human adipose tissue subject to long-term cryopreservation: positive implications for adult stem cell-based therapeutics in patients of advanced age. *Stem Cells Int* 2015; **2015**: 146421 [PMID: 25945096 DOI: 10.1155/2015/146421]

14 **Zuk PA**, Zhu M, Mizuno H, Huang J, Futrell JW, Katz AJ, Benhaim P, Lorenz HP, Hedrick MH. Multilineage cells from human adipose tissue: implications for cell-based therapies. *Tissue Eng* 2001; **7**: 211-228 [PMID: 11304456 DOI: 10.1089/107632701300062859]

15 **Cvetković VJ**, Najdanović JG, Vukelić-Nikolić MĐ, Stojanović S, Najman SJ. Osteogenic potential of *in vitro* osteo-induced adipose-derived mesenchymal stem cells combined with platelet-rich plasma in an ectopic model. *Int Orthop* 2015; **39**: 2173-2180 [PMID: 26231492 DOI: 10.1007/s00264-015-2929-x]

16 **Najdanović JG**, Cvetković VJ, Stojanović S, Vukelić-Nikolić MĐ, Stanisavljević MN, Živković JM, Najman SJ. The influence of adipose-derived stem cells induced into endothelial cells on ectopic vasculogenesis and osteogenesis. *Cell Mol Bioeng* 2015; **8**: 577-590 [DOI: 10.1007/s12195-015-0403-x]

17 **Stojanović S**, Najman S, Korać A. Stem Cells Derived from Lipoma and Adipose Tissue-Similar Mesenchymal Phenotype but Different Differentiation Capacity Governed by Distinct Molecular Signature. *Cells* 2018; **7**: 260 [PMID: 30544806 DOI: 10.3390/cells7120260]

18 **Mushahary D**, Spittler A, Kasper C, Weber V, Charwat V. Isolation, cultivation, and characterization of human mesenchymal stem cells. *Cytometry A* 2018; **93**: 19-31 [PMID: 29072818 DOI: 10.1002/cyto.a.23242]

19 **Shah AR**, Cornejo A, Guda T, Sahar DE, Stephenson SM, Chang S, Krishnegowda NK, Sharma R, Wang HT. Differentiated adipose-derived stem cell cocultures for bone regeneration in polymer scaffolds in vivo. *J Craniofac Surg* 2014; **25**: 1504-1509 [PMID: 24943502 DOI: 10.1097/SCS.0000000000000755]

20 **Cornejo A**, Sahar DE, Stephenson SM, Chang S, Nguyen S, Guda T, Wenke JC, Vasquez A, Michalek JE, Sharma R, Krishnegowda NK, Wang HT. Effect of adipose tissue-derived osteogenic and endothelial cells on bone allograft osteogenesis and vascularization in critical-sized calvarial defects. *Tissue Eng Part A* 2012; **18**: 1552-1561 [PMID: 22440012 DOI: 10.1089/ten.tea.2011.0515]

21 **Du J**, Xie P, Lin S, Wu Y, Zeng D, Li Y, Jiang X. Time-Phase Sequential Utilization of Adipose-Derived Mesenchymal Stem Cells on Mesoporous Bioactive Glass for Restoration of Critical Size Bone Defects. *ACS Appl Mater Interfaces* 2018; **10**: 28340-28350 [PMID: 30080385 DOI: 10.1021/acsami.8b08563]

22 **Zhang H**, Zhou Y, Zhang W, Wang K, Xu L, Ma H, Deng Y. Construction of vascularized tissue-engineered bone with a double-cell sheet complex. *Acta Biomater* 2018; **77**: 212-227 [PMID: 30017924 DOI: 10.1016/j.actbio.2018.07.024]

23 **Papadimitropoulos A**, Scherberich A, Güven S, Theilgaard N, Crooijmans HJ, Santini F, Scheffler K, Zallone A, Martin I. A 3D *in vitro* bone organ model using human progenitor cells. *Eur Cell Mater* 2011; **21**: 445-458; discussion 458 [PMID: 21604244 DOI: 10.22203/ecm.v021a33]

24 **Piattelli M**, Favero GA, Scarano A, Orsini G, Piattelli A. Bone reactions to anorganic bovine bone (Bio-Oss) used in sinus augmentation procedures: a histologic long-term report of 20 cases in humans. *Int J Oral Maxillofac Implants* 1999; **14**: 835-840 [PMID: 10612920]

25 **Živković JM**, Najman SJ, Vukelić MĐ, Stojanović S, Aleksić MV, Stanisavljević MN, Najdanović JG. Osteogenic effect of inflammatory macrophages loaded onto mineral bone substitute in subcutaneous implants. *Arch Biol Sci* 2015; **67**: 173-186 [DOI: 10.2298/ABS140915020Z]

26 **Hoff J**. Methods of blood collection in the mouse. *Lab Animal* 2000; **29**: 47-53

27 **Intini G**, Andreana S, Intini FE, Buhite RJ, Bobek LA. Calcium sulfate and platelet-rich plasma make a novel osteoinductive biomaterial for bone regeneration. *J Transl Med* 2007; **5**: 13 [PMID: 17343737 DOI: 10.1186/1479-5876-5-13]

28 **Murphy MB**, Blashki D, Buchanan RM, Fan D, De Rosa E, Shah RN, Stupp SI, Weiner BK,

Simmons PJ, Ferrari M, Tasciotti E. Multi-composite bioactive osteogenic sponges featuring mesenchymal stem cells, platelet-rich plasma, nanoporous silicon enclosures, and Peptide amphiphiles for rapid bone regeneration. *J Funct Biomater* 2011; **2**: 39-66 [PMID: 24956163 DOI: 10.3390/jfb2020039]

29 **Man Y**, Wang P, Guo Y, Xiang L, Yang Y, Qu Y, Gong P, Deng L. Angiogenic and osteogenic potential of platelet-rich plasma and adipose-derived stem cell laden alginate microspheres. *Biomaterials* 2012; **33**: 8802-8811 [PMID: 22981779 DOI: 10.1016/j.biomaterials.2012.08.054]

30 **Najdanović JG**, Cvetković VJ, Stojanović S, Vukelić-Nikolić MĐ, Čakić-Milošević MM, Živković JM, Najman SJ. Effects of bone tissue engineering triad components on vascularization process: comparative gene expression and histological evaluation in an ectopic bone-forming model. *Biotechnol Biotecnol Equip* 2016; **30**: 1122-1131 [DOI: 10.1080/13102818.2016.1213662]

31 **Najdanović JG**, Cvetković VJ, Vukelić-Nikolić MĐ, Stojanović S, Živković JM, Najman SJ. Vasculogenic potential of adipose-derived mesenchymal stem cells *in vitro* induced into osteoblasts applied with platelet-rich plasma in an ectopic osteogenic model. *Acta Med Median* 2019; **58**: 57-65

32 **Helder MN**, Knippenberg M, Klein-Nulend J, Wuisman PI. Stem cells from adipose tissue allow challenging new concepts for regenerative medicine. *Tissue Eng* 2007; **13**: 1799-1808 [PMID: 17518736 DOI: 10.1089/ten.2006.0165]

33 **Seyed Jafari SM**, Hunger RE. IHC Optical Density Score: A New Practical Method for Quantitative Immunohistochemistry Image Analysis. *Appl Immunohistochem Mol Morphol* 2017; **25**: e12-e13 [PMID: 27093452 DOI: 10.1097/PAI.0000000000000370]

34 **Jahne B**. Practical handbook on image processing for scientific applications. Boca Raton: CRC Press, 1997: 76-82

35 **Varghese F**, Bukhari AB, Malhotra R, De A. IHC Profiler: an open source plugin for the quantitative evaluation and automated scoring of immunohistochemistry images of human tissue samples. *PLoS One* 2014; **9**: e96801 [PMID: 24802416 DOI: 10.1371/journal.pone.0096801]

36 **Bai Y**, Sha J, Kanno T, Miyamoto K, Hideshima K, Matsuzaki Y. Comparison of the Bone Regenerative Capacity of Three-Dimensional Uncalcined and Unsintered Hydroxyapatite/Poly-d/l-Lactide and Beta-Tricalcium Phosphate Used as Bone Graft Substitutes. *J Invest Surg* 2019; 1-14 [PMID: 31122080 DOI: 10.1080/08941939.2019.1616859]

37 **Zilkens C**, Lögters T, Bittersohl B, Krauspe R, Lensing-Höhn S, Jäger M. Spinning around or stagnation - what do osteoblasts and chondroblasts really like? *Eur J Med Res* 2010; **15**: 35-43 [PMID: 20159670 DOI: 10.1186/2047-783X-15-1-35]

38 **Konno M**, Hamazaki TS, Fukuda S, Tokuhara M, Uchiyama H, Okazawa H, Okochi H, Asashima M. Efficiently differentiating vascular endothelial cells from adipose tissue-derived mesenchymal stem cells in serum-free culture. *Biochem Biophys Res Commun* 2010; **400**: 461-465 [PMID: 20708604 DOI: 10.1016/j.bbrc.2010.08.029]

39 **Vogel JP**, Szalay K, Geiger F, Kramer M, Richter W, Kasten P. Platelet-rich plasma improves expansion of human mesenchymal stem cells and retains differentiation capacity and *in vivo* bone formation in calcium phosphate ceramics. *Platelets* 2006; **17**: 462-469 [PMID: 17074722 DOI: 10.1080/09537100600758867]

40 **Liu Y**, Zhou Y, Feng H, Ma GE, Ni Y. Injectable tissue-engineered bone composed of human adipose-derived stromal cells and platelet-rich plasma. *Biomaterials* 2008; **29**: 3338-3345 [PMID: 18485475 DOI: 10.1016/j.biomaterials.2008.04.037]

41 **Lu Y**, Lin N, Chen Z, Xu R. Hypoxia-induced secretion of platelet-derived growth factor-BB by hepatocellular carcinoma cells increases activated hepatic stellate cell proliferation, migration and expression of vascular endothelial growth factor-A. *Mol Med Rep* 2015; **11**: 691-697 [PMID: 25333351 DOI: 10.3892/mmr.2014.2689]

42 **Rolny C**, Nilsson I, Magnusson P, Armulik A, Jakobsson L, Wentzel P, Lindblom P, Norlin J, Betsholtz C, Heuchel R, Welsh M, Claesson-Welsh L. Platelet-derived growth factor receptor-beta promotes early endothelial cell differentiation. *Blood* 2006; **108**: 1877-1886 [PMID: 16690964 DOI: 10.1182/blood-2006-04-014894]

43 **Beckermann BM**, Kallifatidis G, Groth A, Frommhold D, Apel A, Mattern J, Salnikov AV, Moldenhauer G, Wagner W, Diehlmann A, Saffrich R, Schubert M, Ho AD, Giese N, Büchler MW, Friess H, Büchler P, Herr I. VEGF expression by mesenchymal stem cells contributes to angiogenesis in pancreatic carcinoma. *Br J Cancer* 2008; **99**: 622-631 [PMID: 18665180 DOI: 10.1038/sj.bjc.6604508]

44 **Abdel-Malak NA**, Mofarrahi M, Mayaki D, Khachigian LM, Hussain SN. Early growth response-1 regulates angiopoietin-1-induced endothelial cell proliferation, migration, and differentiation. *Arterioscler Thromb Vasc Biol* 2009; **29**: 209-216 [PMID: 19112164 DOI: 10.1161/ATVBAHA.108.181073]

45 **Silverman ES**, Collins T. Pathways of Egr-1-mediated gene transcription in vascular biology. *Am J Pathol* 1999; **154**: 665-670 [PMID: 10079243 DOI: 10.1016/S0002-9440(10)65312-6]

46 **Gashler A**, Sukhatme VP. Early growth response protein 1 (Egr-1): prototype of a zinc-finger family of transcription factors. *Prog Nucleic Acid Res Mol Biol* 1995; **50**: 191-224 [PMID: 7754034 DOI: 10.1016/S0079-6603(08)60815-6]

47 **Fu M**, Zhu X, Zhang J, Liang J, Lin Y, Zhao L, Ehrengruber MU, Chen YE. Egr-1 target genes in human endothelial cells identified by microarray analysis. *Gene* 2003; **315**: 33-41 [PMID: 14557062 DOI: 10.1016/S0378-1119(03)00730-3]

48 **Lyden D**, Hattori K, Dias S, Costa C, Blaikie P, Butros L, Chadburn A, Heissig B, Marks W, Witte L,

Wu Y, Hicklin D, Zhu Z, Hackett NR, Crystal RG, Moore MA, Hajjar KA, Manova K, Benezra R, Rafii S. Impaired recruitment of bone-marrow-derived endothelial and hematopoietic precursor cells blocks tumor angiogenesis and growth. *Nat Med* 2001; **7**: 1194-1201 [PMID: 11689883 DOI: 10.1038/nm1101-1194]

49 **Clauss M**, Weich H, Breier G, Knies U, Röckl W, Waltenberger J, Risau W. The vascular endothelial growth factor receptor Flt-1 mediates biological activities. Implications for a functional role of placenta growth factor in monocyte activation and chemotaxis. *J Biol Chem* 1996; **271**: 17629-17634 [PMID: 8663424 DOI: 10.1074/jbc.271.30.17629]

50 **Sawano A**, Iwai S, Sakurai Y, Ito M, Shitara K, Nakahata T, Shibuya M. Flt-1, vascular endothelial growth factor receptor 1, is a novel cell surface marker for the lineage of monocyte-macrophages in humans. *Blood* 2001; **97**: 785-791 [PMID: 11157498 DOI: 10.1182/blood.V97.3.785]

51 **Michiels C**. Endothelial cell functions. *J Cell Physiol* 2003; **196**: 430-443 [PMID: 12891700 DOI: 10.1002/jcp.10333]

52 **Feuerbach D**, Feyen JH. Expression of the cell-adhesion molecule VCAM-1 by stromal cells is necessary for osteoclastogenesis. *FEBS Lett* 1997; **402**: 21-24 [PMID: 9013850 DOI: 10.1016/s0014-5793(96)01495-0]

53 **Garmy-Susini B**, Jin H, Zhu Y, Sung RJ, Hwang R, Varner J. Integrin alpha4beta1-VCAM-1-mediated adhesion between endothelial and mural cells is required for blood vessel maturation. *J Clin Invest* 2005; **115**: 1542-1551 [PMID: 15902308 DOI: 10.1172/JCI23445]

54 **Starke RD**, Ferraro F, Paschalaki KE, Dryden NH, McKinnon TA, Sutton RE, Payne EM, Haskard DO, Hughes AD, Cutler DF, Laffan MA, Randi AM. Endothelial von Willebrand factor regulates angiogenesis. *Blood* 2011; **117**: 1071-1080 [PMID: 21048155 DOI: 10.1182/blood-2010-01-264507]

55 **Lee J**, Lee S, Ahmad T, Madhurakkat Perikamana SK, Lee J, Kim EM, Shin H. Human adipose-derived stem cell spheroids incorporating platelet-derived growth factor (PDGF) and bio-minerals for vascularized bone tissue engineering. *Biomaterials* 2020; **255**: 120192 [PMID: 32559565 DOI: 10.1016/j.biomaterials.2020.120192]

56 **Silverman MD**, Zamora DO, Pan Y, Texeira PV, Planck SR, Rosenbaum JT. Cell adhesion molecule expression in cultured human iris endothelial cells. *Invest Ophthalmol Vis Sci* 2001; **42**: 2861-2866 [PMID: 11687530]

57 **Shibuya M**, Claesson-Welsh L. Signal transduction by VEGF receptors in regulation of angiogenesis and lymphangiogenesis. *Exp Cell Res* 2006; **312**: 549-560 [PMID: 16336962 DOI: 10.1016/j.yexcr.2005.11.012]

58 **Abhinand CS**, Raju R, Soumya SJ, Arya PS, Sudhakaran PR. VEGF-A/VEGFR2 signaling network in endothelial cells relevant to angiogenesis. *J Cell Commun Signal* 2016; **10**: 347-354 [PMID: 27619687 DOI: 10.1007/s12079-016-0352-8]

59 **Cui Q**, Dighe AS, Irvine JN Jr. Combined angiogenic and osteogenic factor delivery for bone regenerative engineering. *Curr Pharm Des* 2013; **19**: 3374-3383 [PMID: 23432677 DOI: 10.2174/1381612811319190004]

60 **Olsson AK**, Dimberg A, Kreuger J, Claesson-Welsh L. VEGF receptor signalling - in control of vascular function. *Nat Rev Mol Cell Biol* 2006; **7**: 359-371 [PMID: 16633338 DOI: 10.1038/nrm1911]

61 **Carmeliet P**, Jain RK. Molecular mechanisms and clinical applications of angiogenesis. *Nature* 2011; **473**: 298-307 [PMID: 21593862 DOI: 10.1038/nature10144]

62 **Mayer H**, Bertram H, Lindenmaier W, Korff T, Weber H, Weich H. Vascular endothelial growth factor (VEGF-A) expression in human mesenchymal stem cells: autocrine and paracrine role on osteoblastic and endothelial differentiation. *J Cell Biochem* 2005; **95**: 827-839 [PMID: 15838884 DOI: 10.1002/jcb.20462]

63 **Midy V**, Plouët J. Vasculotropin/vascular endothelial growth factor induces differentiation in cultured osteoblasts. *Biochem Biophys Res Commun* 1994; **199**: 380-386 [PMID: 8123039 DOI: 10.1006/bbrc.1994.1240]

64 **Tombran-Tink J**, Barnstable CJ. Osteoblasts and osteoclasts express PEDF, VEGF-A isoforms, and VEGF receptors: possible mediators of angiogenesis and matrix remodeling in the bone. *Biochem Biophys Res Commun* 2004; **316**: 573-579 [PMID: 15020256 DOI: 10.1016/j.bbrc.2004.02.076]

65 **Street J**, Bao M, deGuzman L, Bunting S, Peale FV Jr, Ferrara N, Steinmetz H, Hoeffel J, Cleland JL, Daugherty A, van Bruggen N, Redmond HP, Carano RA, Filvaroff EH. Vascular endothelial growth factor stimulates bone repair by promoting angiogenesis and bone turnover. *Proc Natl Acad Sci USA* 2002; **99**: 9656-9661 [PMID: 12118119 DOI: 10.1073/pnas.152324099]

66 **Park S**, DiMaio TA, Scheef EA, Sorenson CM, Sheibani N. PECAM-1 regulates proangiogenic properties of endothelial cells through modulation of cell-cell and cell-matrix interactions. *Am J Physiol Cell Physiol* 2010; **299**: C1468-C1484 [PMID: 20810911 DOI: 10.1152/ajpcell.00246.2010]

67 **Givens C**, Tzima E. Endothelial Mechanosignaling: Does One Sensor Fit All? *Antioxid Redox Signal* 2016; **25**: 373-388 [PMID: 27027326 DOI: 10.1089/ars.2015.6493]

68 **Ribatti D**, Tamma R, Ruggieri S, Annese T, Crivellato E. Surface markers: An identity card of endothelial cells. *Microcirculation* 2020; **27**: e12587 [PMID: 31461797 DOI: 10.1111/micc.12587]

69 **Bourin P**, Bunnell BA, Casteilla L, Dominici M, Katz AJ, March KL, Redl H, Rubin JP, Yoshimura K, Gimble JM. Stromal cells from the adipose tissue-derived stromal vascular fraction and culture expanded adipose tissue-derived stromal/stem cells: a joint statement of the International Federation for Adipose Therapeutics and Science (IFATS) and the International Society for Cellular Therapy (ISCT). *Cytotherapy* 2013; **15**: 641-648 [PMID: 23570660 DOI: 10.1016/j.jcyt.2013.02.006]

70 **Ebrahimian TG**, Pouzoulet F, Squiban C, Buard V, André M, Cousin B, Gourmelon P, Benderitter M, Casteilla L, Tamarat R. Cell therapy based on adipose tissue-derived stromal cells promotes physiological and pathological wound healing. *Arterioscler Thromb Vasc Biol* 2009; **29**: 503-510 [PMID: 19201690 DOI: 10.1161/ATVBAHA.108.178962]

71 **Barradas AM**, Yuan H, van Blitterswijk CA, Habibovic P. Osteoinductive biomaterials: current knowledge of properties, experimental models and biological mechanisms. *Eur Cell Mater* 2011; **21**: 407-429; discussion 429 [PMID: 21604242 DOI: 10.22203/ecm.v021a31]

72 **Detsch R**, Mayr H, Ziegler G. Formation of osteoclast-like cells on HA and TCP ceramics. *Acta Biomater* 2008; **4**: 139-148 [PMID: 17723325 DOI: 10.1016/j.actbio.2007.03.014]

73 **Ripamonti U**, Roden LC. Induction of bone formation by transforming growth factor-beta2 in the non-human primate Papio ursinus and its modulation by skeletal muscle responding stem cells. *Cell Prolif* 2010; **43**: 207-218 [PMID: 20546239 DOI: 10.1111/j.1365-2184.2010.00675.x]

74 **Chai YC**, Carlier A, Bolander J, Roberts SJ, Geris L, Schrooten J, Van Oosterwyck H, Luyten FP. Current views on calcium phosphate osteogenicity and the translation into effective bone regeneration strategies. *Acta Biomater* 2012; **8**: 3876-3887 [PMID: 22796326 DOI: 10.1016/j.actbio.2012.07.002]

75 **Barba-Recreo P**, Del Castillo Pardo de Vera JL, Georgiev-Hristov T, Ruiz Bravo-Burguillos E, Abarrategi A, Burgueño M, García-Arranz M. Adipose-derived stem cells and platelet-rich plasma for preventive treatment of bisphosphonate-related osteonecrosis of the jaw in a murine model. *J Craniomaxillofac Surg* 2015; **43**: 1161-1168 [PMID: 26027865 DOI: 10.1016/j.jcms.2015.04.026]

76 **Yadav MC**, Simão AM, Narisawa S, Huesa C, McKee MD, Farquharson C, Millán JL. Loss of skeletal mineralization by the simultaneous ablation of PHOSPHO1 and alkaline phosphatase function: a unified model of the mechanisms of initiation of skeletal calcification. *J Bone Miner Res* 2011; **26**: 286-297 [PMID: 20684022 DOI: 10.1002/jbmr.195]

77 **Huitema LF**, Apschner A, Logister I, Spoorendonk KM, Bussmann J, Hammond CL, Schulte-Merker S. Entpd5 is essential for skeletal mineralization and regulates phosphate homeostasis in zebrafish. *Proc Natl Acad Sci USA* 2012; **109**: 21372-21377 [PMID: 23236130 DOI: 10.1073/pnas.1214231110]

78 **Inazumi M**, Takekawa M, Oka K, Shibayama N. Effects of adipose tissue-derived stem cells transplanted to a bone defect after irradiation. *J Hard Tissue Biology* 2020; **29**: 111-122 [DOI: 10.2485/jhtb.29.111]

79 **Yeh HI**, Lee PY, Su CH, Tian TY, Ko YS, Tsai CH. Reduced expression of endothelial connexins 43 and 37 in hypertensive rats is rectified after 7-day carvedilol treatment. *Am J Hypertens* 2006; **19**: 129-135 [PMID: 16448880 DOI: 10.1016/j.amjhyper.2005.08.020]

80 **Guillotin B**, Bareille R, Bourget C, Bordenave L, Amédée J. Interaction between human umbilical vein endothelial cells and human osteoprogenitors triggers pleiotropic effect that may support osteoblastic function. *Bone* 2008; **42**: 1080-1091 [PMID: 18387350 DOI: 10.1016/j.bone.2008.01.025]

81 **Bronckers AL**, Gay S, Finkelman RD, Butler WT. Immunolocalization of Gla proteins (osteocalcin) in rat tooth germs: comparison between indirect immunofluorescence, peroxidase-antiperoxidase, avidin-biotin-peroxidase complex, and avidin-biotin-gold complex with silver enhancement. *J Histochem Cytochem* 1987; **35**: 825-830 [PMID: 3298423 DOI: 10.1177/35.8.3298423]

82 **Chenu C**, Colucci S, Grano M, Zigrino P, Barattolo R, Zambonin G, Baldini N, Vergnaud P, Delmas PD, Zallone AZ. Osteocalcin induces chemotaxis, secretion of matrix proteins, and calcium-mediated intracellular signaling in human osteoclast-like cells. *J Cell Biol* 1994; **127**: 1149-1158 [PMID: 7962073 DOI: 10.1083/jcb.127.4.1149]

83 **Santos MI**, Reis RL. Vascularization in bone tissue engineering: physiology, current strategies, major hurdles and future challenges. *Macromol Biosci* 2010; **10**: 12-27 [PMID: 19688722 DOI: 10.1002/mabi.200900107]

84 **Clarkin CE**, Garonna E, Pitsillides AA, Wheeler-Jones CP. Heterotypic contact reveals a COX-2-mediated suppression of osteoblast differentiation by endothelial cells: A negative modulatory role for prostanoids in VEGF-mediated cell: cell communication? *Exp Cell Res* 2008; **314**: 3152-3161 [PMID: 18718465 DOI: 10.1016/j.yexcr.2008.07.027]

85 **Collin-Osdoby P**, Rothe L, Bekker S, Anderson F, Huang Y, Osdoby P. Basic fibroblast growth factor stimulates osteoclast recruitment, development, and bone pit resorption in association with angiogenesis *in vivo* on the chick chorioallantoic membrane and activates isolated avian osteoclast resorption in vitro. *J Bone Miner Res* 2002; **17**: 1859-1871 [PMID: 12369790 DOI: 10.1359/jbmr.2002.17.10.1859]

86 **Bouletreau PJ**, Warren SM, Spector JA, Peled ZM, Gerrets RP, Greenwald JA, Longaker MT. Hypoxia and VEGF up-regulate BMP-2 mRNA and protein expression in microvascular endothelial cells: implications for fracture healing. *Plast Reconstr Surg* 2002; **109**: 2384-2397 [PMID: 12045566 DOI: 10.1097/00006534-200206000-00033]

87 **Kozawa O**, Matsuno H, Uematsu T. Involvement of p70 S6 kinase in bone morphogenetic protein signaling: vascular endothelial growth factor synthesis by bone morphogenetic protein-4 in osteoblasts. *J Cell Biochem* 2001; **81**: 430-436 [PMID: 11255225 DOI: 10.1002/1097-4644(20010601)81:3<430::aid-jcb1056>3.0.co;2-g]

88 **Cai X**, Su X, Li G, Wang J, Lin Y. Osteogenesis of adipose-derived stem cells. In: Lin Y. Osteogenesis. Rijeka, Croatia: IntechOpen, 2012: 135-152 [DOI: 10.5772/34025]

89 **Reinholt FP**, Hultenby K, Oldberg A, Heinegård D. Osteopontin--a possible anchor of osteoclasts to bone. *Proc Natl Acad Sci USA* 1990; **87**: 4473-4475 [PMID: 1693772 DOI: 10.1073/pnas.87.12.4473]

90 **Hyun JS**, Nelson ER, Montoro D, Levi B, Longaker MT. Skeletal and adipose tissue engineering with adipose-derived stromal cells. In: Eberli D. Tissue engineering for tissue and organ regeneration. Rijeka, Croatia: IntechOpen, 2011: 107-128 [DOI: 10.5772/22971]

91 **Yoshimi R**, Yamada Y, Ito K, Nakamura S, Abe A, Nagasaka T, Okabe K, Kohgo T, Baba S, Ueda M. Self-assembling peptide nanofiber scaffolds, platelet-rich plasma, and mesenchymal stem cells for injectable bone regeneration with tissue engineering. *J Craniofac Surg* 2009; **20**: 1523-1530 [PMID: 19816290 DOI: 10.1097/SCS.0b013e3181b09b7e]

92 **Anitua E**, Andia I, Ardanza B, Nurden P, Nurden AT. Autologous platelets as a source of proteins for healing and tissue regeneration. *Thromb Haemost* 2004; **91**: 4-15 [PMID: 14691563 DOI: 10.1160/TH03-07-0440]

93 **Marx RE**. Platelet-rich plasma: evidence to support its use. *J Oral Maxillofac Surg* 2004; **62**: 489-496 [PMID: 15085519 DOI: 10.1016/j.joms.2003.12.003]

94 **Vukelić-Nikolić MĐ**, Najman SJ, Vasiljević PJ, Jevtović-Stoimenov TM, Cvetković VJ, Andrejev MN, Mitić ŽJ. Osteogenic capacity of diluted platelet-rich plasma in ectopic bone-forming model: Benefits for bone regeneration. *J Craniomaxillofac Surg* 2018; **46**: 1911-1918 [PMID: 30309795 DOI: 10.1016/j.jcms.2018.09.005]

95 **Yang H**, Hong N, Liu H, Wang J, Li Y, Wu S. Differentiated adipose-derived stem cell cocultures for bone regeneration in RADA16-I in vitro. *J Cell Physiol* 2018; **233**: 9458-9472 [PMID: 29995982 DOI: 10.1002/jcp.26838]

96 **Peng H**, Wright V, Usas A, Gearhart B, Shen HC, Cummins J, Huard J. Synergistic enhancement of bone formation and healing by stem cell-expressed VEGF and bone morphogenetic protein-4. *J Clin Invest* 2002; **110**: 751-759 [PMID: 12235106 DOI: 10.1172/JCI15153]

97 **Li G**, Corsi-Payne K, Zheng B, Usas A, Peng H, Huard J. The dose of growth factors influences the synergistic effect of vascular endothelial growth factor on bone morphogenetic protein 4-induced ectopic bone formation. *Tissue Eng Part A* 2009; **15**: 2123-2133 [PMID: 19215221 DOI: 10.1089/ten.tea.2008.0214]

98 **Helmrich U**, Di Maggio N, Güven S, Groppa E, Melly L, Largo RD, Heberer M, Martin I, Scherberich A, Banfi A. Osteogenic graft vascularization and bone resorption by VEGF-expressing human mesenchymal progenitors. *Biomaterials* 2013; **34**: 5025-5035 [PMID: 23566801 DOI: 10.1016/j.biomaterials.2013.03.040]

Published by **Baishideng Publishing Group Inc**
7041 Koll Center Parkway, Suite 160, Pleasanton, CA 94566, USA
Telephone: +1-925-3991568
E-mail: bpgoffice@wjgnet.com
Help Desk: https://www.f6publishing.com/helpdesk
https://www.wjgnet.com